



HAL
open science

Anticancer Properties of Indole Derivatives as IsoCombretastatin A-4 analogues

Shannon Pecnard, Abdallah Hamze, Jérôme Bignon, Bastien Prost, Alain Deroussent, Laura Gallego-Yerga, Rafael Peláez, Ji Yeon Paik, Marc Diederich, Mouâd Alami, et al.

► **To cite this version:**

Shannon Pecnard, Abdallah Hamze, Jérôme Bignon, Bastien Prost, Alain Deroussent, et al.. Anticancer Properties of Indole Derivatives as IsoCombretastatin A-4 analogues. *European Journal of Medicinal Chemistry*, 2021, 223, pp.113656. 10.1016/j.ejmech.2021.113656 . hal-03349143

HAL Id: hal-03349143

<https://hal.science/hal-03349143v1>

Submitted on 20 Sep 2021

HAL is a multi-disciplinary open access archive for the deposit and dissemination of scientific research documents, whether they are published or not. The documents may come from teaching and research institutions in France or abroad, or from public or private research centers.

L'archive ouverte pluridisciplinaire **HAL**, est destinée au dépôt et à la diffusion de documents scientifiques de niveau recherche, publiés ou non, émanant des établissements d'enseignement et de recherche français ou étrangers, des laboratoires publics ou privés.

Anticancer Properties of Indole Derivatives as *IsoCombretastatin A-4* analogues

Shannon Pecnard,^a Abdallah Hamze,^{*a} Jérôme Bignon,^b Bastien Prost,^c Alain Deroussent^d
Laura Gallego-Yerga,^e Rafael Peláez,^e Ji Yeon Paik,^f Marc Diederich,^f Mouad Alami,^{*a} and
Olivier Provot^{*a}

^a *Université Paris-Saclay, CNRS, BioCIS, 92290, Châtenay-Malabry, France.*

^b *Institut de Chimie des Substances Naturelles, UPR 2301, CNRS avenue de la terrasse, F-91198 Gif sur Yvette, France.*

^c *Service d'Analyse des Médicaments et Métabolites, IPSIT, Univ. Paris-Sud, UMS 3679 CNRS, US 31 INSERM, Université Paris-Saclay, 92290 Châtenay Malabry, France.*

^d *Metabolic and Systemic aspects of oncogenesis (METSU), UMR 9018, CNRS, Institut Gustave Roussy, Université Paris-Saclay, 94805 Villejuif. France.*

^e *Laboratorio de Química Orgánica y Farmacéutica, Departamento de Ciencias Farmacéuticas, Facultad de Farmacia, Universidad de Salamanca, Salamanca, Spain.*

^f *Department of Pharmacy, College of Pharmacy, Seoul National University, 1 Gwanak-ro, Gwanak-gu, Seoul 08626, Korea.*

^{*} *Corresponding authors. Tel.: +33 1 46 83 58 47. Fax: +33 1 46 83 58 28. Email: olivier.provot@universite-paris-saclay.fr mouad.alami@universite-paris-saclay.fr and abdallah.hamze@universite-paris-saclay.fr*

Abstract

In this study, a variety of original ligands related to Combretastatin A-4 and *isoCombretastatin A-4*, able to inhibit the tubulin polymerization into microtubules, was designed, synthesized, and evaluated. Our lead compound **15d** having a quinazoline as A-ring and a 2-substituted indole as B-ring separated by a *N*-methyl linker displayed a remarkable sub-nanomolar level of cytotoxicity (IC₅₀ < 1 nM) against 9 human cancer cell lines.

Keywords: Cancer, cytotoxicity, indole, *isoCA-4*, oxazinoindole, pyridoindole, quinazoline, tubulin.

1. Introduction

Isolated from the African willow tree, *Combretum caffrum* by G. Pettit[1] in 1989, Combretastatin A-4 (CA-4 **1**, Figure 1) is a very potent cytotoxic agent having nanomolar IC_{50} values against many human cancer cell lines.[2] This (*Z*)-stilbene acts by binding to the colchicine site on β -tubulin, thus interrupting the polymerization of tubulin into microtubules.[3] Moreover, it has been demonstrated that a moderate single dose of CA-4P **2**, a water-soluble phosphate pro-drug of CA-4, causes almost complete cessation of the blood circulation in tumour vessels without vascular damage in normal cells.[4,5,6] This discovery was the source of a spectacular craze from the scientific community for this small molecule which was then the subject of numerous structure-activity relationships studies.[7,8,9] The majority of these structural modifications consisted in introducing the (*Z*)-double bond into cyclic or heterocyclic systems since it has been shown that, despite its pronounced efficacy in clinical trials, the (*Z*)-double bond of CA-4 isomerizes during storage, administration and metabolism leading to the more stable but less active *E*-isomer.[10,11,12] In the continuation of our work dedicated to the synthesis of non-isomerizable analogues of CA-4[13], we discovered that the stable synthetic compound *iso*CA-4 **3**, displayed the same anti-cancer activities as its natural isomer CA-4 but without the risk of isomerization.[14,15,16,17] We next demonstrated that several modifications of the phenolic B-ring of CA-4 and *iso*CA-4 were authorized by introducing, for example $-NH_2$, $-alkynes$, $-alkenyl$ groups, or a fluorine atom in place of the C3'-OH substituent.[18,19] We and the Pinney's group have also showed that the ethylene double bond of *iso*CA-4 can be reduced[20] or inserted into cycles and heterocycles[21,22,23,24,25,26] without loss of anti-cancer properties. Structure-activity relationships (SARs) also revealed that various non-isomerizable linkers of small size are welcome[13] of which the *N*-Methyl group predominated (*e.g.*, *azaFisoerianin* **4**).[27] Finally, it was demonstrated that the classical 3,4,5-trimethoxyphenyl (TMP) A-ring of CA-4 and *iso*CA-4 could be advantageously replaced by heterocycles as quinazolines[28] or quinolines[29] to promote highly cytotoxic analogues **6**[30] and **7**[31] having in structures a carbazole nucleus as B-ring. Herein, we were interested in synthesizing and evaluating the cytotoxicity of target molecules of type pyrido[1,2-*a*]indoles **11**[32] depicted in Scheme 1, which could be seen as analogues of carbazole compounds **5-7**[33,34] by connecting the nitrogen atom N1 to the carbon atom C2 in the carbazole system. We will also evaluate the cytotoxicity of their 6,9-dihydropyrido[1,2-*a*]indole precursors **10** to understand the structure-activity relationships (SARs) better. Next, the insertion of an oxygen atom in the pyridine part of the pyrido[1,2-*a*]indoles ring of compounds **11** leading to oxazino[4,3-*a*]indoles **12** (Scheme 2) and their "opened" analogues **15** (Schemes 3 and 4) will be presented by establishing a comprehensive SAR study.

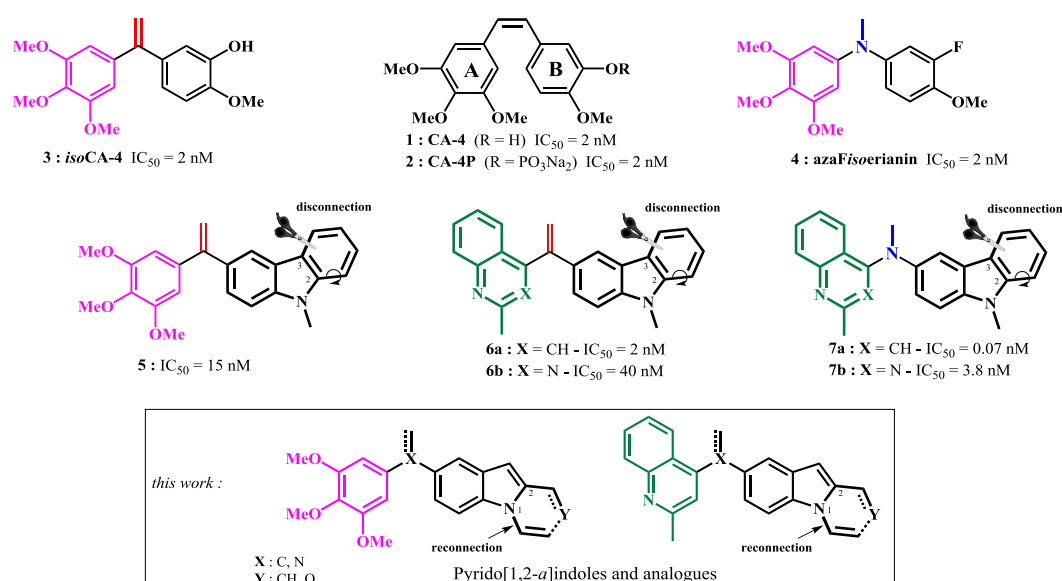
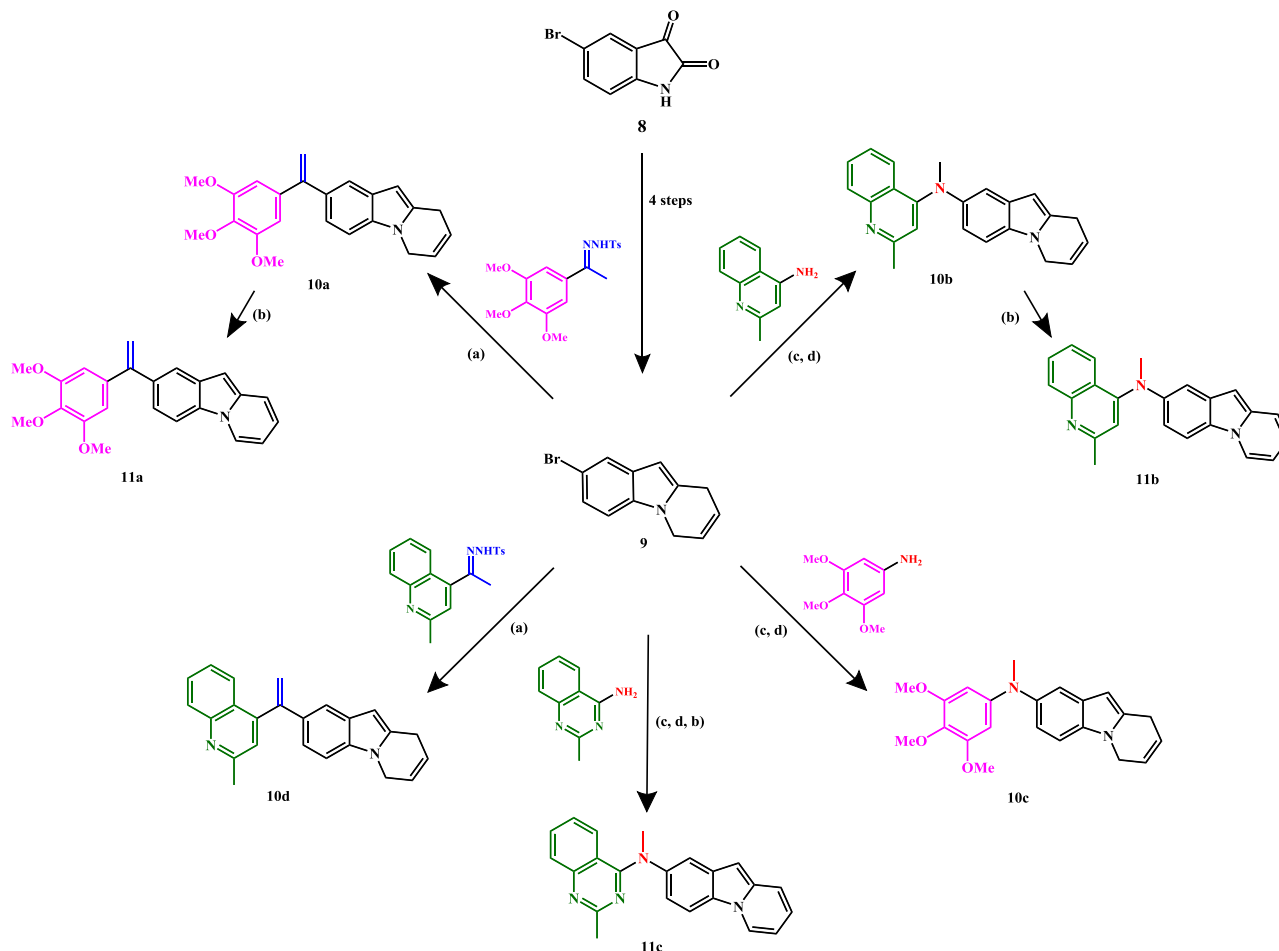


Figure 1. Structures of CA-4 **1**, CA-4P **2** and a selection of analogues **3-7** accompanied by target molecules pyrido[1,2-*a*]indoles.

2. Results and discussion

2.1. Chemistry.

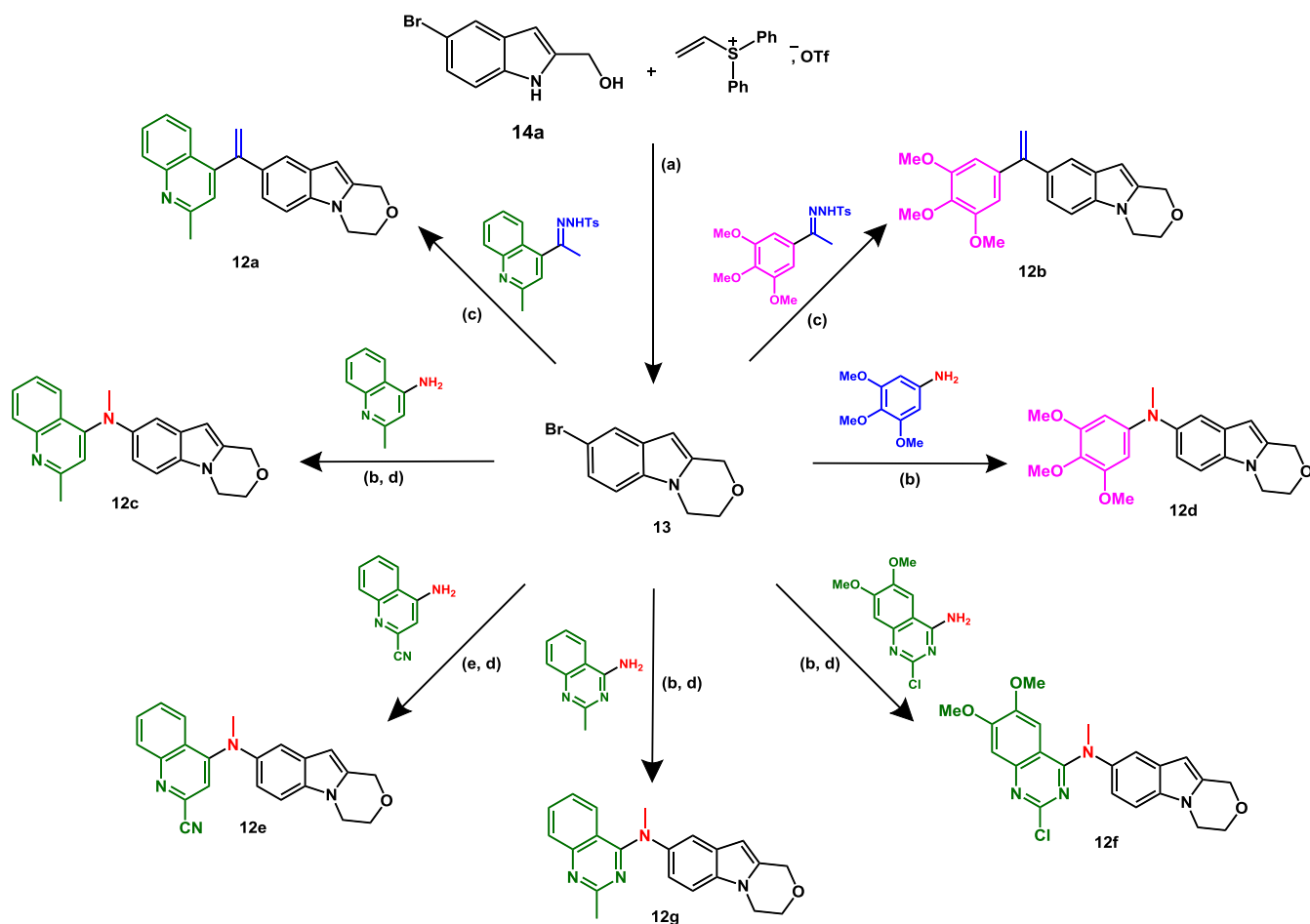


Reagents and conditions: (a) Pd₂dba₃·CHCl₃, XPhos, LiOtBu, dioxane, 100 °C. (b) Pd/C 10 mol%, xylene, 145 °C, 24 h. (c) Pd₂dba₃·CHCl₃, XPhos, NaOtBu, dioxane, 100 °C. (d) NaH, CH₃I, DMF, rt.

Scheme 1. Synthesis of targets pyridinoindoles **11a-c** and reduced analogues **10a-d**.

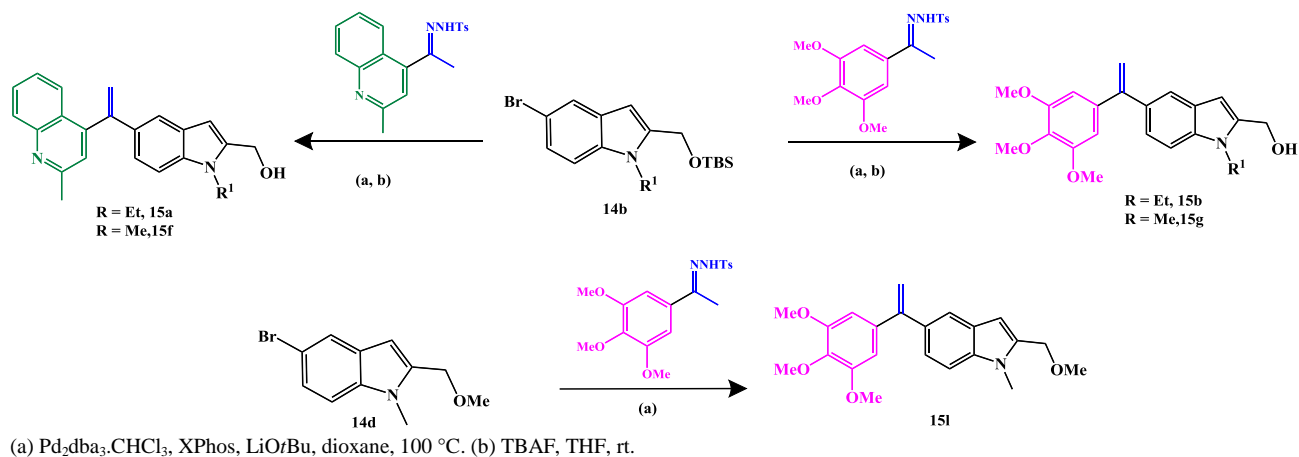
To synthesize 6,9-dihydropyridino[1,2-*a*]indoles **10** and pyridino[1,2-*a*]indole targets **11**, we first prepare the brominated building block **9** as the key intermediate starting from 5-bromoindolin-3-one in four steps (Scheme 1).^[35] Compound **11a** was obtained in two steps from the coupling reaction between **9** and the *N*-tosylhydrazone of 3,4,5-trimethoxyphenylacetophenone to provide **10a**.^[36] Then, 6,9-dihydropyridino[1,2-*a*]indole **10a** was oxidized into **11a** using Pd/C in hot xylene. Amino derivative **11b** was obtained from **9** which was successfully coupled with 4-aminoquinoline to give after a *N*-methylation reaction **10b** finally oxidized into pyridino[1,2-*a*]indole **11b**. The brominated platform **9** was also successfully used to provide in two steps **10c** and **10d** in a similar manner as described for above for **10b** and **10a** respectively. Finally, quinazoline derivative **11c** bearing a pyridino[1,2-*a*]indole B-ring, a quinazoline A-ring and a *N*-methyl group as linker was prepared in three steps from 4-aminoquinazoline and **9** under Buchwald-Hartwig conditions without isolating the synthetic intermediates which revealed to be partially unstable on silica gel column.

Next, we prepared a series of 3,4-dihydro-1*H*-[1,4]oxazino[4,3-*a*]indoles **12a-g** having a *N*-methyl or an ethylene linker and various A-ring as quinolines, quinazolines and the traditional 3,4,5-trimethoxyphenyl ring. (Scheme 2). The key brominated intermediate 8-bromo-3,4-dihydro-1*H*-[1,4]oxazino[4,3-*a*]indole **13**, useful for coupling reactions, was prepared from indole **14a** according to a slightly modified procedure described by Chen and Xiao.^[37] By replacing



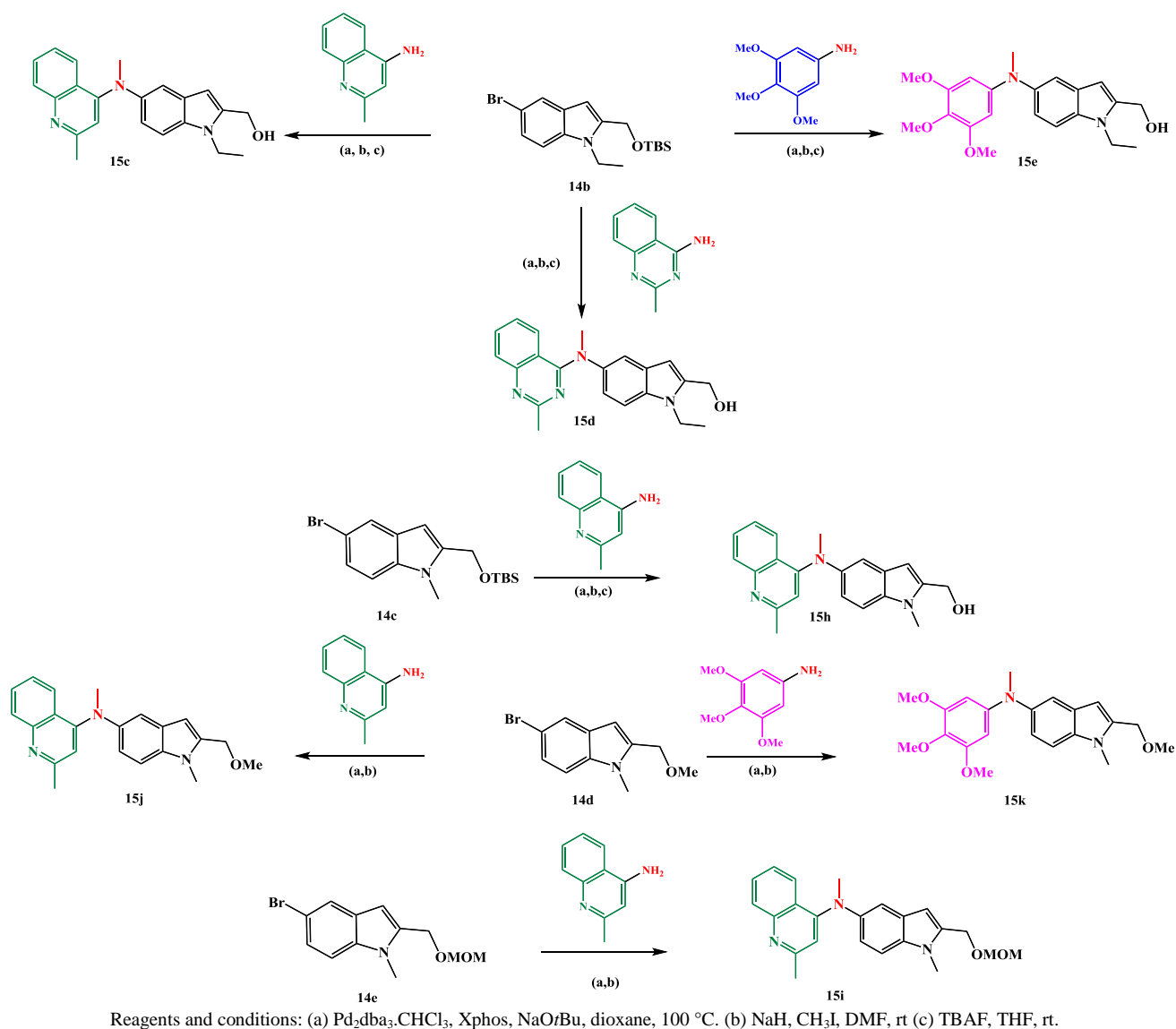
Scheme 2. Synthesis of targets 3,4-dihydro-1H-[1,4]oxazino[4,3-a]indoles **12a-g**.

KOH with NaH as the base and CH₂Cl₂ by fluorobenzene as the solvent, the reaction between (5-bromo-1H-indol-2-yl)methanol **14a** and diphenyl vinyl sulfonium triflate led to **13** in only 30 min with a 92 % yield (for comparison when using KOH in CH₂Cl₂, **13** was obtained after 10 h of reaction with a 76 % yield). Then, 8-bromo-3,4-dihydro-1H-[1,4]oxazino[4,3-a]indole **13** was successfully coupled with hydrazino derivatives under Pd-catalysis to give **12a** and **12b** with good yields (82% and 62%, respectively). For the synthesis of compound **12e** having a nitrile group, the same catalytic system was used as before but Cs₂CO₃ was employed as a base instead of LiOtBu to avoid a CN-hydration reaction.[38] The tertiary amines **12c-g** were obtained after a *N*-methylation reaction (without isolating the intermediate secondary diarylamines) with variable yields (from 30% to 75% for the two steps).



Scheme 3. Synthesis of target indole compounds **15** having an ethylene linker.

We also prepared for biological comparisons, a series of 1,2-disubstituted indole derivatives **15a-l** as “opened analogues” of oxazino[4,3-*a*]indoles **12** (Schemes 3 and 4). Diarylethylene compounds **15a,b** and **15f,g** were prepared in two steps from the Barluenga’s coupling reactions between the brominated platforms **14b** or **14c** with the required *N*-tosylhydrazones followed by a *O*-desilylation reaction using TBAF in THF (Scheme 3). Diarylmethylamines **15c-e** were prepared in three steps according to a Buchwald coupling reaction using above reaction conditions with **14b** and *N*-ethylindoles, and the required secondary amines were then *N*-methylated and *O*-deprotected without prior purification (Scheme 4). *N*-methylindole **15h** having on C2 a CH₂OH-substituent was prepared similarly after a three steps sequence (Buchwald-Hardwig coupling, *N*-methylation and desilylation). *N*-methylindoles **15j,k** having on C2 a CH₂OMe group were prepared according to a Buchwald-Harding coupling reaction followed by a *N*-methylation reaction as above. Finally, indole derivative **15i** having on C2 a CH₂OMOM-group was prepared in two steps from 5-bromo-2-(methoxymethyl)-1-methyl-1*H*-indole **14e** and 4-aminoquinoline. It is important to note that all secondary amine and silylated intermediates were used without needing to be purified.



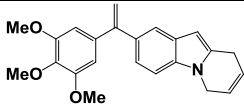
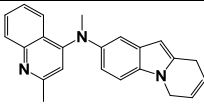
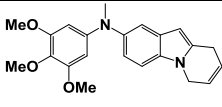
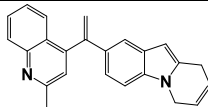
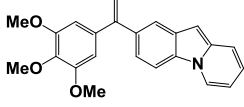
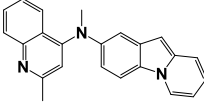
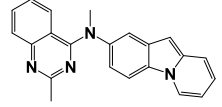
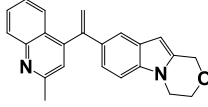
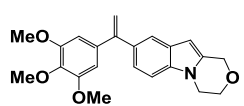
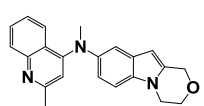
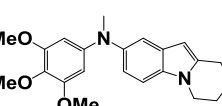
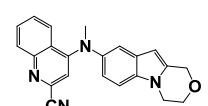
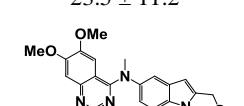
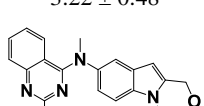
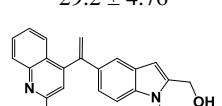
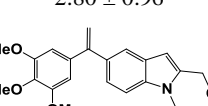
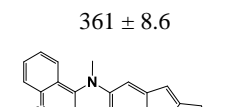
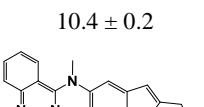
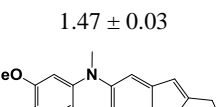
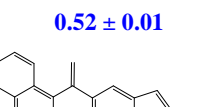
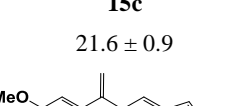
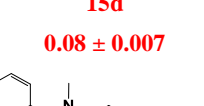
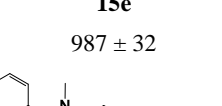
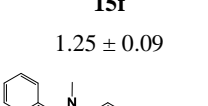
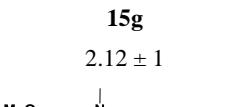
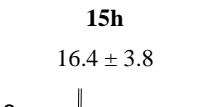
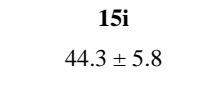
Scheme 4. Synthesis of target indole compounds **15** having a *N*-methyl linker

2.2. Biology.

2.2.1. Cytotoxicity of new compounds against HCT116 cells

In vitro cytotoxicity of the synthesized 6,9-dihydropyrido[1,2-*a*]indoles **10a-d**, pyrido[1,2-*a*]indoles **11a-d**, dihydro-1*H*-[1,4]oxazino[4,3-*a*]indoles **12a-g** as well as 2-substituted indoles **15a-l** was evaluated against HCT116 human colon

Table 1 Cytotoxicity against HCT116 cells^a and ITP of new compounds **10**, **11**, **12** and **15**.

Compounds				
IC ₅₀ ^b [nM]	970 ± 39.7	5.2 ± 0.1	959 ± 37	25.7 ± 1.24
Compounds				
IC ₅₀ ^b [nM]	213 ± 17.5	78.4 ± 9.6	6.87 ± 0.34	109 ± 2.9
Compounds				
IC ₅₀ ^b [nM]	23.5 ± 11.2	3.22 ± 0.48	29.2 ± 4.76	2.80 ± 0.96
Compounds				
IC ₅₀ ^b [nM]	361 ± 8.6	10.4 ± 0.2	1.47 ± 0.03	0.52 ± 0.01
Compounds				
IC ₅₀ ^b [nM]	21.6 ± 0.9	0.08 ± 0.007	987 ± 32	1.25 ± 0.09
Compounds				
IC ₅₀ ^b [nM]	2.12 ± 1	16.4 ± 3.8	44.3 ± 5.8	10.2 ± 0.39
Compounds				
IC ₅₀ ^b [nM]	47.5 ± 2.42	72.4 ± 2.2	0.64 ± 0.03	

^a HCT116 human colon carcinoma ^b IC₅₀ is the concentration of compound needed to reduce cell growth by 50% following 72 h cell treatment with the tested drug (average of three experiments).

carcinoma (HCT116) cell line. A fluorimetry-based assay was used to determine of the drug concentration required to inhibit cell growth by 50% after incubation in the culture medium for 72 h. *IsoCA-4*[39] was included as the reference compound for comparisons. Examination of compounds **10a-d** in which the 6,9-dihydropyridino[1,2-*a*]indole B-ring was constant showed that derivative **10b** (IC₅₀ = 5.2 nM) having a quinoline as A-ring and a *N*-Methyl linker was undoubtedly the most active compound in this series. Replacing the quinoline with the isosteric TMP nucleus considerably reduced the cytotoxicity level against HCT116 cancer cells (**10c**, IC₅₀ = 959 nM), similarly, the replacement of the *N*-methyl linker present in **10b** by a 1,1-ethylene linker decreased cytotoxicity by a five-fold factor (**10d**, IC₅₀ = 25.7 nM). Pyrido[1,2-*a*]indoles **11a-c**, which were the first compounds targeted in this study as structural analogues of carbazoles (Figure 1) displayed varying toxicity levels. Comparison of **11b** (IC₅₀ = 78.4 nM) with **10b** (IC₅₀ = 5.2 nM) showed that the aromatization of the 6,9-dihydropyridino[1,2-*a*]indole nucleus decreased the cytotoxicity level. We can also note that pyrido[1,2-*a*]indole **11b** was found to be significantly less cytotoxic than its

carbazole analogue **7b**.^[29] However, we were pleased to observe that, in the pyrido[1,2-*a*]indoles series, the quinaldine A-ring replacement with a quinazoline motif increased the cytotoxic activity 11-fold (compare **11b** with **11c**). Next, compounds **12a-g** were examined and compared from a biological point of view. Again, in this class of compounds having a 3,4-dihydro-1*H*-[1,4]oxazino[4,3-*a*]indole as B-ring, the two more potent drugs **12c** (IC₅₀ = 3.22 nM) and **12e** (IC₅₀ = 2.80 nM) have in structure a 2-substituted quinoline as ring A and an *N*-methyl linker. Examining the cytotoxicity level of **12g** (IC₅₀ = 10.4 nM) revealed that a 2-methylquinazoline nucleus as A-ring was also well-tolerated in this series. The replacement of these heterocycles by the “classical” TMP A-ring present in **12b** (IC₅₀ = 23.5 nM) and **12d** (IC₅₀ = 29.2 nM) caused a slight decrease in cytotoxicity against HCT116 cells. Finally, results depicted in Table 1 suggest that compounds **15** having a 2-substituted indole as B-ring are the more cytotoxic compounds of this study, with five compounds displaying a cytotoxicity level ranging from 0.08 nM to 2.12 nM. Examination of Table 1 also revealed that compounds having as B-ring a C2-hydroxymethylindole and an ethylene linker tolerated well as A-ring a quinaldine (**15a** IC₅₀ = 1.47 nM) or a TMP nucleus (**15b** IC₅₀ = 0.52 nM; **15g** IC₅₀ = 2.12 nM). With compounds having the same indolic B-ring and a *N*-methyl linker, results depicted in Table 1 showed that the best A-ring was a quinazoline, with our lead compound **15d** having a remarkable IC₅₀ value of 0.08 nM. The replacement of a quinazoline by a quinaldine in these compounds led to a slight decrease in cytotoxicity (**15c** IC₅₀ = 21.6 nM; **15h** IC₅₀ = 16.4 nM) and led to a dramatic loss of activity by changing these heterocycles by a TMP ring (**15e** IC₅₀ = 978 nM).^[40] Comparison of the cytotoxicity level of compounds **15h**, **15i** and **15j** revealed that the methylation of the alcohol function led to equipotent drugs (compare **15h** IC₅₀ = 16.4 nM and **15j** IC₅₀ = 10.2 nM) whereas a -CH₂OMOM substituent on C2 of the indole decreased the activity (**15i** IC₅₀ = 44.3 nM). In this preliminary screening, we found 16 compounds of different structures having a cytotoxicity level inferior to 30 nM. Before studying the mechanism of action of the most promising compounds in this series, we performed comparative metabolization studies of the two most cytotoxic compounds **15b** and **15d** against HCT116 cells in the presence of rats and human microsomes.

2.2.2 *In vitro* metabolisation study of **15b** and **15d** vs *isoCA-4*.^[17]

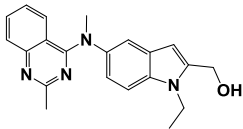
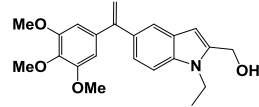
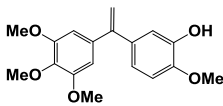
2.2.2.1 Characterization of **15d**, **15b**, *isoCA-4* and metabolites by HPLC-MS.

High resolution electrospray mass spectra (HRMS/ESI⁺) of compounds **15b**, **15d** and *isoCA-4* provided their protonated molecular ions [M+H]⁺ at *m/z* 347.1863 (347.1872 calculated for C₂₁H₂₃N₄O), *m/z* 368.1854 (368.1862 calculated for C₂₂H₂₆NO₄) and *m/z* 317.1384 (317.1389 calculated for C₁₈H₂₁O₅), respectively. After 96 h incubation with rat or human liver microsomes, compound **15d** could produce minor *N*-demethylated metabolites and hydroxylated metabolites, although **15b** compound and *isoCA-4* were mainly metabolized into *O*-demethylated (M-14) and hydroxylated metabolites as described before.^[30]

2.2.2.2. Microsomal stability of studied compounds

To determine their metabolic stability, expressed as the percentage (%) of remaining parent compound concentration over time, kinetic monitoring was performed by HPLC-MS/MS of independent incubations of each compound with rat liver microsomes (RLM) and human liver microsomes (HLM). Concentrations of each compound in microsomal incubations were backcalculated using their calibration curves. After quantification of the ratio of the residual concentration to its initial value, the half-life time was 18 h for *isoCA-4*, 70 h for **15b**, and 140 h for **15d** with rat liver microsomes (Table 2). The half-life time was 30 h for *isoCA-4*, 89 h for **15b** and 145 h for **15d** with human liver microsomes (as shown in Table 2). It is of note that these *in vitro* t_{1/2} values for each drug are observed in good agreement between rat and human liver microsomes. The natural logarithms (ln) of the remaining concentrations (%) were plotted against incubation times (Figures 2a and 2b). Using the value 3.912 of (ln 50), the *in vitro* half-lives (t_{1/2}) were found with HLM in the following ascending order, *isoCA-4* < **15b** < **15d**, in agreement with this obtained with

Table 2. Metabolic stability of *isoCA-4*, quinazoline **15d** and **15b** in rat liver microsomes (RLM) and human liver microsomes (HLM)

Compound structure	Half-life time (h) ^a	Half-life time (h) ^a
	(Rat liver microsomes)	(Human liver microsomes)
 15d	140 ± 15	145 ± 15
 15b	70 ± 5	89 ± 5
 <i>isoCA-4</i>	18 ± 2	30 ± 3

^aThe metabolic stability is expressed as the in vitro half-life time, based on the 3,912 value (ln 50) corresponding to the remaining concentration.

RLM. However, a slower metabolism was observed with HLM than with RLM. The quinazoline compound **15d** showed the best metabolic stability when compared with *isoCA-4*.

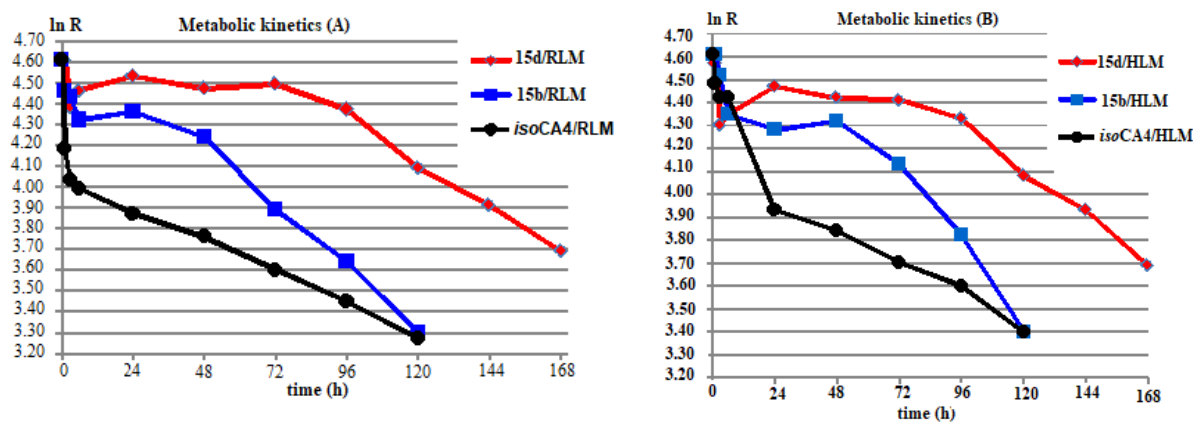


Figure 2. Metabolic stability profiles of *isoCA-4*, **15d** and **15b** derivatives in rat liver microsomes (A) and in human liver microsomes (B).

2.2.3 Inhibition of tubulin polymerization for selected compounds

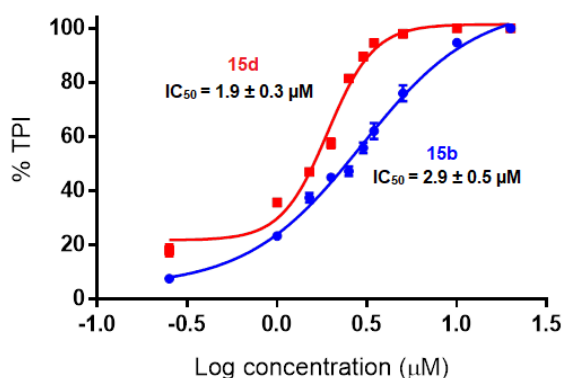


Figure 3. Effect of compounds **15b** (blue line) and **15d** (red line) on tubulin polymerization. Tubulin polymerization inhibition (TPI) is indicated in percentage. The polymerization percentage was calculated, for each concentration, by comparing the amplitude of tubulin-ligand curves from 4 °C to 37 °C with the amplitude observed for the negative control, considered as 100% of polymerization. Results are expressed as mean ± SEM of three independent experiments.

To investigate whether cytotoxic compounds **15b** and **15d** were exerting their activities by interacting with microtubules, their effects on *in vitro* polymerization of tubulin were examined using porcine brain tubulin, which was isolated following Shelanski's procedure.[41] As it can be seen in Figure 3, the selected compounds inhibited tubulin polymerization with micromolar IC₅₀ values. It is of note that the concentrations required to inhibit tubulin polymerization using **15b** and **15d** (IC₅₀ at a micromolar level) are much higher than those required for cytotoxicity and similar observations have been previously noticed in many other classes of antimetabolic agents, including epithilones,[42] paclitaxel,[43] and *isoCA-4* analogues prepared in our group.

2.2.4 Cytotoxicity of **15d** against eight other human cancer cells

According to the metabolism and TPI results, we next decided to evaluate our lead compound **15d** on eight other tumor cell lines: human glioblastoma (U87-MG), human lung epithelial (A549), human breast adenocarcinoma (MDA-MB231), Human pancreatic carcinoma (MiaPACA2), Human lung cancer (HT1080), Chronic myeloid leukemia cells (K562), Doxorubicin-resistant chronic myeloid leukemia cells (K562R)[44] and Human colorectal adenocarcinoma cells (HT29). The results of this study are depicted in Table 3.

Table 3. Cytotoxicity against, U87-MG, A549, MDA-MB231, MiaPACA2, K562, K562R and HT29 human cancer cell lines.

Compounds	U87-MG ^b	A549 ^c	MDA-MB231 ^d	MiaPACA2 ^e	HT1080 ^f	K562 ^g	K562R ^h	HT29 ⁱ
IC ₅₀ ^a [nM] 15d	0.51 ± 0.009	0.70 ± 0.02	0.25 ± 0.02	0.09 ± 0.005	0.08 ± 0.1	0.26 ± 0.03	0.10 ± 0.02	0.84 ± 0.14
IC ₅₀ [nM] <i>isoCA-4</i>	8.24 ± 0.9	52.7 ± 6.7	1.98 ± 0.6	3.01 ± 0.1	0.91 ± 0.07	4.26 ± 0.5	5.13 ± 0.04	> 100

^a IC₅₀ is the concentration of **15d** needed to reduce cell growth by 50% following 72 h cell treatment with the tested drug (average of three experiments). ^b U87 Human glioblastoma cells. ^c A549, Human lung epithelial cells. ^d MDA-MB231 Human breast adenocarcinoma cells. ^e MiaPACA2 Human pancreatic carcinoma cells. ^f HT1080 Human lung cancer cells. ^g K562 Chronic myeloid leukemia cells. ^h K562R Doxorubicin-resistant chronic myeloid leukemia cells. ⁱ HT29 Human colorectal adenocarcinoma cells.

2.2.5. Effect of **15d** on cell cycle.

Indole derivative **15d** which displayed against all cancer cell lines a sub-nanomolar cytotoxicity level was next tested in dose-response experiments on K562 cell cycle distribution. K562 cells were treated for 24 h with increasing concentrations of **15d** and DMSO was used as control. As seen in Fig. 4, **15d**, at a concentration of 0.5 nM has arrested

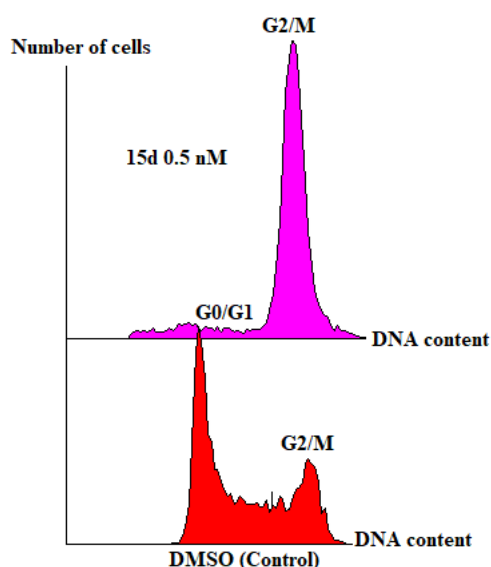


Figure 4. Effect of **15d** on cell cycle distribution in K562 cells determined by flow cytometry analysis. DNA content was assessed *via* propidium iodide staining.

the entire population of K562 cells in the G2/M phase of the cellular cycle. It is important to note that the cellular cycle blockade in the G2/M phase at such a low concentration has never been reported for *isoCA-4* and analogues.

2.2.6 Effects of **15d** on mitochondrial dysfunction in K562 Cells

Mitochondria play critical roles in cellular metabolism, homeostasis, and stress responses by generating ATP for energy and regulating cell death.[45] Mitochondrial dysfunction is usually caused by depolarization and is the early hallmark of toxicity mediated through caspase-induced apoptosis.[46] As shown in Figure 5, **15d** induced mitochondrial dysfunction was detected using a fluorescence-based mitochondria-specific voltage-dependent dye, JC-1 assay. Thus, these results showed that **15d** induced mitochondrial dysfunction in a concentration-dependent manner, with significant effects beginning at a very low concentration of 0.5 nM. Our study provides convincing evidence indicating that compound **15d** dose-dependently caused caspase-induced apoptosis of K562 cells through mitochondrial dysfunction.

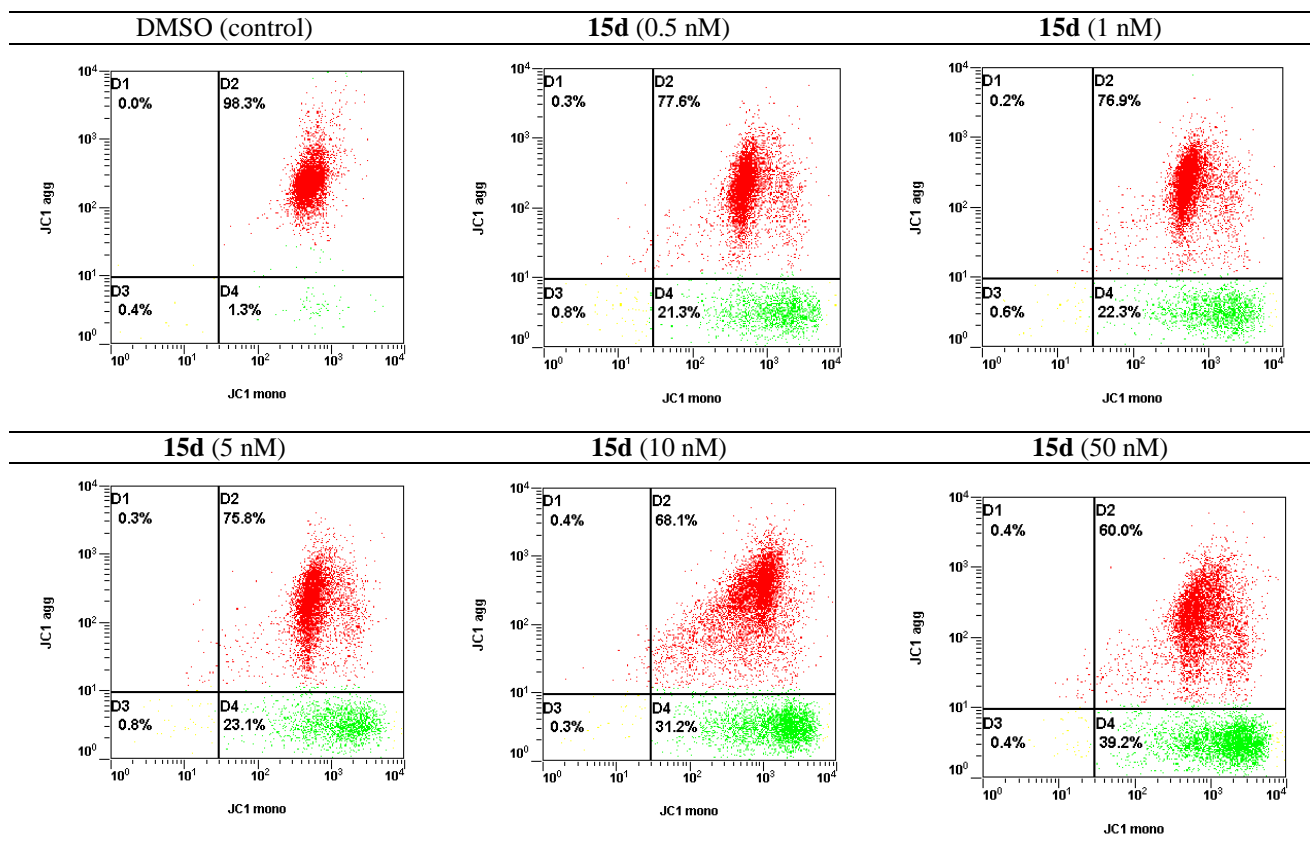
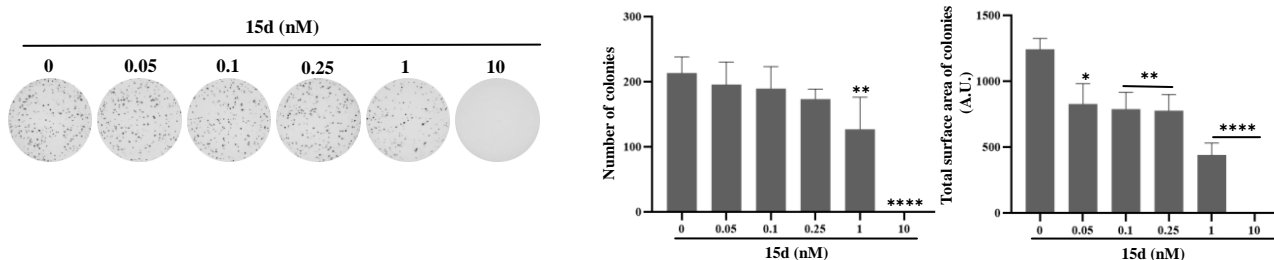


Figure 5 Compound **15d** induced mitochondrial dysfunction in K562 leukemia cells. Cells were incubated with **15d** at concentrations from 0.5 to 50 nM for 48 h at 37 °C. The portion of mitochondria dysfunction was measured using the JC1 assay.

2.2.7 Inhibition of colony formation in K562 and imatinib-resistant K562 cells by **15d**

We next quantified the inhibition of the clonogenic potential by **15d** in a 3D culture environment using Methocult colony formation assays (CFA). **15d** significantly reduced the number, total surface area and average size of K562 and imatinib resistant K562IR cell colonies (Figure 6).

(A) K562 cells



(B) K562IR cells

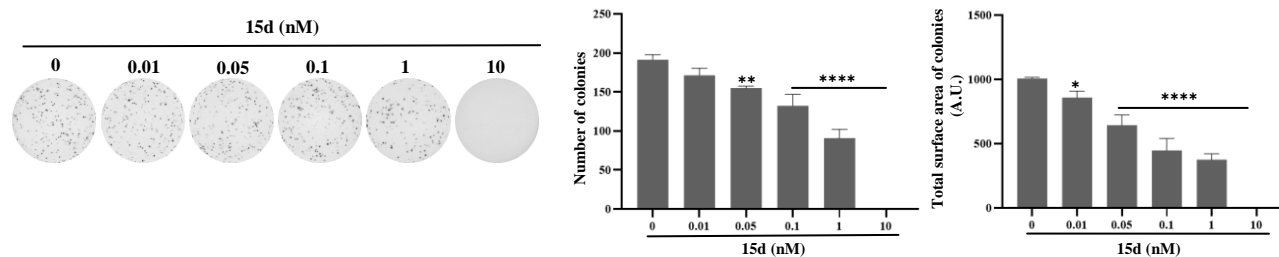


Figure 6. Representative pictures from three independent experiments of clonogenic assays after treatment with **15d** (A) K562, (B) K562IR. Quantifications (number of colonies and the total surface area of colonies) are indicated. Statistical analysis was performed by two-way ANOVA, followed by Tukey's multiple comparisons test. Differences were considered significant when * $p < 0.05$, ** $p < 0.01$, *** $p < 0.001$ compared to control. n/s: not significant.

2.3. Molecular modelling

Figure 7a presents the results of molecular docking calculations for compound **15d** within the colchicine binding site of tubulin β subunit (the structure obtained from X-ray crystal structure with accession code 6H9B).[30] The overall binding mode observed match that previously reported for *isoCA-4* (see overlay on Figure 7b) and for compound **6b**,[28] where the quinazoline nucleus was accommodated in the lipophilic pocket ordinarily occupied by the trimethoxyphenyl A-ring. Interactions that can be expected given this binding mode hypothesis include notably (see Figure 6a) three potential hydrogen bonds between (i) the side-chain SH group of the cysteine $\beta 241$ residue and the N1 atom of the quinazoline moiety (ii) the primary O-H function (hydrogen bond donor) of the indole with the carbonyl of backbone's asparagine $\beta 350$ (iii) the O-H (hydrogen bond acceptor) with the NH of backbone's valine $\beta 315$.

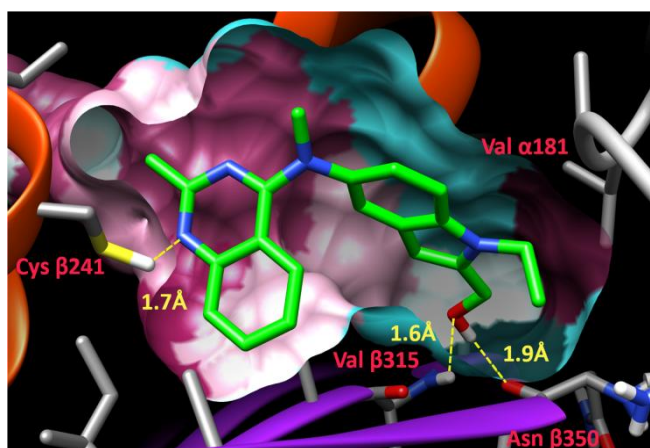


Figure 7a Putative binding mode of **15d** (green) within colchicine binding site of tubulin X-ray structure (accession code 6H9B) showing expected hydrogen bonds between ligand atoms and cysteine $\beta 241$ and valine $\beta 315$.

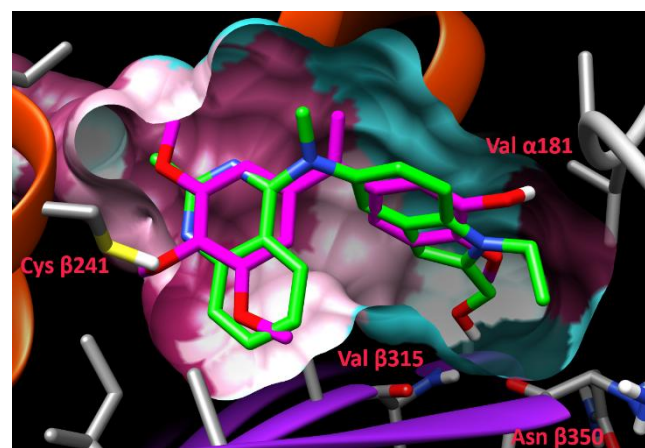


Figure 7b Docked pose of **15d** (green) overlaid with *isoCA-4* (fushia) in the tubulin binding site.

3. Conclusion

Overall, we have presented efficient syntheses of various original *isoCA-4* analogues having as B-rings pyridoindoles, oxazinoindoles, and indoles nucleus. Among the 26 compounds synthesized, a large majority showed excellent cytotoxicity levels that can be compared to CA-4 and *isoCA-4* as references. Compound **15d**, which has a quinazoline as ring A, a 2-substituted indole as ring B, and a *N*-Methyl linker has proven to be the most promising compound of these different series. Indole-quinazoline compound **15d** shows excellent cytotoxicity on 9 human cancer cell lines at a sub-nanomolar level that *has never been observed in this research area*. Moreover, it was observed that this compound

presents a remarkable efficacy on K562R Doxorubicin-resistant chronic myeloid leukemia cell lines. This compound, which inhibits tubulin assembly into microtubules at a classic micromolar level, shows a very interesting metabolic stability, making it a promising drug candidate. Cell cycle studies have revealed that **15d** blocks this cycle in the G2/M phase at a very low concentration of 0.5 nM, a concentration at which **15d** also induced an important mitochondrial dysfunction. Interestingly, indole **15d** was showed to significantly reduced the number, total surface area and average size of K562 and K562IR cell colonies in a dose-dependent manner. Finally, docking studies show that **15d** adopts a similar orientation to that of *isoCA-4* when bound to β -tubulin by establishing 3 stabilizing hydrogen bonds.

From a therapeutic point of view, it is important to note that compound **15d** is certainly too cytotoxic to be used as *in vivo*. It is therefore appropriate to use this compound, due to its very high cytotoxicity ($IC_{50} \ll 1$ nM) as a payload in an antibody-drug conjugate (ADC) strategy, as reported recently with CA-4.[47] Moreover, **15d** could also be included in squalene nanoparticles, as shown in our lab with *isoCA-4*[48] for an improved efficacy, or in liposomal formulations. Further studies are currently underway in the lab to determine this compound's full potential for further development.

4. Experimental

4.1 General considerations

Solvent peaks were used as reference values, with $CDCl_3$ at 7.26 ppm for 1H NMR and 77.16 ppm for ^{13}C NMR, with $(CD_3)_2CO$ at 2.05 ppm for 1H NMR and 29.84 ppm for ^{13}C NMR, and with $DMSO-d_6$ at 2.50 ppm for 1H NMR and 39.5 ppm for ^{13}C NMR. Chemical shifts δ are given in parts per million, and the following abbreviations are used: singlet (s), doublet (d), doublet of doublet (dd), triplet (t), td (triplet of doublet), ddd (doublet of doublet of doublet), multiplet (m) and broad singlet (bs). Reaction courses and product mixtures were routinely monitored by TLC on silica gel, and compounds were visualized with UV light (254nm) or by solution of phosphomolybdic acid/ Δ , anisaldehyde/ Δ , ninhydrine/ Δ or vanillin/ Δ . Flash chromatography was performed using silica gel 60 (40–63 mm, 230–400 mesh) at medium pressure (200 mbar). Fluorobenzene was used as received, and dioxane, dichloromethane, cyclohexane, and tetrahydrofuran were classically dried. Organic extracts were, in general, dried over $MgSO_4$ or Na_2SO_4 . High-resolution mass spectra were recorded on a Bruker Daltonics micrOTOF-Q II instrument. All products reported showed 1H and ^{13}C NMR spectra in agreement with the assigned structures. LCMS were done with $H_2O/ACN/0.1\%$ Formic Acid gradient 1-30% 15 min with column Sunfire C18 – 2.1x150mm – 3.5 μ m. IR spectra were measured on a Bruker Vector 22 spectrophotometer (neat, cm^{-1}).

4.2 Procedure for the synthesis of new compounds

4.2.1 General procedure for the Barluenga coupling reaction (protocol A) if necessary followed by a desilylation reaction used for: **10a**, **10d**, **12a**, **12b**, **15a**, **15b**, **15f**, **15g** and **15l**.

A sealed tube under argon atmosphere was charged at room temperature with 1 eq of appropriate 5-bromo-indole derivative (0.2 mmol) (**9**, **13**, **14b**, **14c** and **14d**), 1.2 eq of corresponding *N*-tosylhydrazone (0.24 mmol), $Pd_2dba_3 \cdot CHCl_3$ (5 mol%), XPhos (10 mol%) and 2.4 eq of $LiOtBu$ (0.5 mmol) in dry dioxane. The mixture was then heated at 100 °C until disappearance of bromo indole derivative evaluated by silica TLC (8/2 cyclohexane/ $AcOEt$). The crude mixture was then allowed to room temperature, filtered through Celite pad with ethyl acetate, and the solvents were evaporated under reduced pressure and the crude residue was purified by silica gel chromatography (95/5 to 85/15 of cyclohexane/ $EtOAc$). The crude was then concentrated under vacuum to give a solid (**10a**, **10d**, **12a**, **12b**). For compounds having a O-Si group, the crude residue was dissolved in dry THF with 1.1 eq of TBAF (1M in THF) for 3 h at room temperature. Reaction completion was evaluated by silica TLC (6/4 cyclohexane/ $AcOEt$). After completion, the solvent is evaporated under reduced pressure and the crude residue was purified by silica gel chromatography (90/10 to 70/30 of cyclohexane/ $EtOAc$) to give the product as a solid (**15a**, **15b**, **15f**, **15g** and **15l**).

4.2.2. *General procedure for the Buchwald-Hartwig coupling reaction (protocol B) followed by a N-methylation reaction for 10b, 10c, 11c, 12c, 12d, 12e, 12f, 12g, 15i, 15j and 15k and, for 15c, 15d, 15e and 15h a N-methylation reaction and a desilylation step.*

A sealed tube under argon atmosphere was charged at room temperature with 1 eq of corresponding 5-bromo-indole derivative (0.2 mmol) (**9**, **13**, **14b**, **14c**, **14d**, **14e**), 1.2 eq of appropriate primary amine (0.24 mmol), Pd₂dba₃.CHCl₃ (5 mol%), XPhos (10 mol%) and 1.5 eq (0.3 mmol) of NaOtBu (or Cs₂CO₃ for **12e**) in dry dioxane. The mixture was then heated at 100 °C until disappearance of bromo indole derivative evaluated by silica TLC (7/3 cyclohexane/AcOEt). The crude mixture was then allowed to cool down to room temperature, filtration through Celite, and the solvents were evaporated under reduced pressure. The crude residue was dissolved in freshly distilled DMF (4mL) at 0 °C and 2 eq of NaH were added. After 20 min., 1.2 eq of MeI was slowly added and the mixture was stirred at room temperature for 6 h. Reaction completion was evaluated by silica TLC (6/4 cyclohexane/EtOAc). The reaction was cooled to 0 °C, saturated aqueous NH₄Cl solution was added by small portions and the mixture was extracted with EtOAc. The organic layer was washed with saturated aqueous NH₄Cl solution (2x), saturated aqueous NaHCO₃ solution and brine. The combined organic layers were dried over MgSO₄ and concentrated in vacuum. The crude product was purified by silica gel chromatography (95/5 to 80/20 cyclohexane/EtOAc). The product was then concentrated under vacuum to give a solid (**10b**, **10c**, **12c**, **12d**, **12e**, **12f**, **12g**, **15i**, **15j** and **15k**). For compounds having a OTBS group, the crude residue was dissolved in dry THF with 1.1 eq of TBAF (1M in THF) at room temperature until disappearance of starting material evaluated by silica TLC (6/4 cyclohexane/AcOEt). After completion the solvent was evaporated under reduced pressure and the crude residue was purified by silica gel chromatography (90/10 to 60/40 of cyclohexane/EtOAc) to give the product as a solid (**15c**, **15d**, **15e** and **15h**).

4.2.3. *General aromatization procedure leading to 11a-c (protocol C).*

A sealed tube under argon atmosphere was charged at room temperature with 1 eq of corresponding dihydropyrido indole **10a** or **10b** and Pd/C (20 mol%) in *p*-xylene. The mixture was then heated at 145 °C for 48 h. Reaction completion was evaluated by analytical HPLC. The crude mixture was then allowed to cool down to room temperature, Filtration through Celite, and the solvent was evaporated under reduced pressure. The crude product was purified by inverse phase column on preparative HPLC. The product was then concentrated under vacuum to give compounds **11a** or **11b**. Compound **11c** was obtained after a Buchwald-Hartwig coupling reaction (protocol B) between **9** and 4-aminoquinazoline followed by a *N*-methylation reaction and an oxidation step (as for **11a,b**; protocol C).

4.2.4. *Description of new compounds*

4.2.4.1. *2-(1-(3,4,5-Trimethoxyphenyl)vinyl)-6,9-dihydropyrido[1,2-a]indole 10a*

Protocol A. Column chromatography on silica gel afforded 87 mg of the product as light brown solid (0.24 mmol, yield 60%); TLC (SiO₂, 8/2 cyclohexane/EtOAc); R_f = 0.69; m.p. = 89 °C ¹H NMR (300 MHz, Acetone-d₆) δ 7.49 (d, *J* = 1.0 Hz, 1H), 7.30 (dt, *J* = 8.5, 0.8 Hz, 1H), 7.13 (dd, *J* = 8.5, 1.7 Hz, 1H), 6.66 (s, 2H), 6.25 (d, *J* = 1.0 Hz, 1H), 6.09 (d, *J* = 1.2 Hz, 2H), 5.38 (q, *J* = 1.6 Hz, 2H), 4.75 – 4.56 (m, 2H), 3.77 (s, 3H), 3.75 (s, 6H), 3.60 (dtd, *J* = 6.2, 4.6, 3.9, 2.4 Hz, 2H); ¹³C NMR (75 MHz, Acetone-d₆) δ 154.0 (2C), 152.5, 139.2, 139.1, 136.5, 134.8, 134.0, 129.2, 122.8, 121.7, 121.5, 120.2, 112.3, 109.3, 107.0 (2C), 98.3, 60.6, 56.4 (2C), 42.5, 24.5; IR neat (cm⁻¹): 2934, 1579, 1504, 1412, 1343, 1235, 1125, 1005; HRMS (ESI⁺) for C₂₃H₂₄NO₃ [M + H]⁺: calcd 362.1756 found 362.1753.

4.2.4.2. *N-Methyl-N-(2-methylquinolin-4-yl)-6,9-dihydropyrido[1,2-a]indol-2-amine 10b*

Protocol B followed by a *N*-Methylation reaction. Column chromatography on silica gel afforded 46 mg of the product as yellow solid (0.13 mmol, yield 71%); TLC (SiO₂, 9/1 DCM/MeOH); R_f = 0.58 ; m.p = 84 °C; ¹H NMR (300 MHz, CDCl₃) δ 7.94 (d, *J* = 8.4 Hz, 1H), 7.58 (t, *J* = 7.4 Hz, 1H), 7.52 – 7.40 (m, 1H), 7.28 – 7.18 (m, 1H), 7.18 – 7.10 (m,

1H), 7.02 (dd, $J = 8.5, 6.8$ Hz, 1H), 6.94 – 6.82 (m, 2H), 6.20 (d, $J = 15.9$ Hz, 1H), 6.04 (s, 1H), 6.00 – 5.87 (m, 1H), 4.59 (dd, $J = 5.6, 3.5$ Hz, 2H), 3.71 – 3.51 (m, 2H), 3.49 (s, 3H), 2.72 (s, 3H); ^{13}C NMR (75 MHz, Acetone- d_6) δ 164.2, 158.2, 156.5, 146.9, 144.2, 135.8, 130.4, 126.8, 126.5, 124.8, 122.7, 121.4, 119.9, 118.4, 115.9, 111.1, 109.2, 100.1, 98.3, 45.3, 42.5, 24.5, 23.4; IR (cm^{-1}): 2932, 2920, 1486, 1466, 1362, 1212, 1088, 805, 787; HRMS (ESI $^+$) for $\text{C}_{23}\text{H}_{22}\text{N}_3$ [M + H] $^+$: calcd 340.1808 found 340.1805.

4.2.4.3. *N*-Methyl-*N*-(3,4,5-trimethoxyphenyl)-6,9-dihydropyrido[1,2-*a*]indol-2-amine **10c**

Protocol B followed by a *N*-Methylation reaction. Column chromatography on silica gel afforded 58 mg of the product as a yellow oil (0.16 mmol, yield 57%); TLC (SiO_2 , 7/3 cyclohexane/EtOAc); ^1H NMR (300 MHz, Acetone- d_6) δ 7.35 – 7.27 (m, 2H), 6.97 (dd, $J = 8.6, 2.2$ Hz, 1H), 6.61 (dt, $J = 9.9, 1.9$ Hz, 1H), 6.31 (s, 1H), 6.12 – 5.99 (m, 3H), 4.13 (t, $J = 7.1$ Hz, 2H), 3.67 (s, 6H), 3.64 (s, 3H), 3.28 (s, 3H), 2.66 (tdd, $J = 6.9, 4.4, 1.9$ Hz, 2H); ^{13}C NMR (75 MHz, Acetone- d_6) δ 154.6 (2C), 148.2, 142.9, 136.5, 135.6, 132.2, 130.5, 125.6, 121.4, 120.8, 117.5, 110.4, 100.0 (2C), 95.2, 60.7, 56.3 (2C), 41.6, 40.4, 24.9; IR (cm^{-1}): 3001, 2955, 2254, 1655, 1504, 1412, 1235, 1125, 1005, 797; HRMS (ESI $^+$) for $\text{C}_{22}\text{H}_{25}\text{N}_2\text{O}_3$ [M + H] $^+$: calcd 365.1865 found 365.1858.

4.2.4.4. 2-(1-(2-Methylquinolin-4-yl)vinyl)-6,9-dihydropyrido[1,2-*a*]indole **10d**

Protocol A. Column chromatography on silica gel afforded 71 mg of the product as a light brown solid (0.21 mmol, yield 53%); TLC (SiO_2 , 6/4 cyclohexane/EtOAc); $R_f = 0.66$; m.p. = 129 °C ^1H NMR (300 MHz, Methanol- d_4) δ 7.95 (d, $J = 8.5$ Hz, 1H), 7.72 (d, $J = 8.4$ Hz, 1H), 7.60 (ddd, $J = 8.4, 6.8, 1.5$ Hz, 1H), 7.34 (s, 1H), 7.27 (d, $J = 1.6$ Hz, 1H), 7.24 (dd, $J = 8.4, 1.4$ Hz, 1H), 7.17 (d, $J = 8.6$ Hz, 1H), 7.09 (dd, $J = 8.6, 1.8$ Hz, 1H), 6.06 (s, 1H), 6.00 (s, 2H), 5.95 (d, $J = 1.3$ Hz, 1H), 5.27 (d, $J = 1.3$ Hz, 1H), 4.54 – 4.42 (m, 2H), 3.54 – 3.43 (m, 2H), 2.72 (s, 3H); ^{13}C NMR (75 MHz, Methanol- d_4) δ 160.2, 152.3, 149.1, 148.8, 137.0, 135.5, 133.1, 130.7, 129.9, 128.5, 127.6, 127.0, 126.8, 123.8, 123.1, 121.5, 120.1, 119.2, 115.1, 109.9, 98.6, 42.7, 24.71, 24.65; IR (cm^{-1}): 3044, 2924, 1592, 1485, 1463, 1446, 1393, 1366, 882, 767; HRMS (ESI $^+$) for $\text{C}_{24}\text{H}_{21}\text{N}_2$ [M + H] $^+$: calcd 337.1705 found 337.1700.

4.2.4.5. 2-(1-(3,4,5-Trimethoxyphenyl)vinyl)pyrido[1,2-*a*]indole **11a**

Protocol C. A sealed tube under argon atmosphere was charged at room temperature with 1 eq of **10a** and Pd/C (20 mol%) in *p*-xylene. The mixture was then heated at 145 °C for 48 h. Reaction completion was evaluated by analytical HPLC. The crude mixture was then allowed to cool down to room temperature, filtration through Celite, and the solvent was evaporated under reduced pressure. The crude product was purified by inverse phase column on preparative HPLC to give compound 11mg **11a** as brown oil (0.03 mmol, yield 37%); TLC (SiO_2 , 8/2 Cyclohexane/EtOAc); $R_f = 0.70$; ^1H NMR (300 MHz, Acetone- d_6) δ 8.67 (d, $J = 7.2$ Hz, 1H), 8.08 (d, $J = 8.7$ Hz, 1H), 7.74 (d, $J = 1.7$ Hz, 1H), 7.51 (dt, $J = 9.3, 1.2$ Hz, 1H), 7.27 (dd, $J = 8.7, 1.7$ Hz, 1H), 6.96 (ddd, $J = 9.2, 6.3, 1.1$ Hz, 1H), 6.66 (s, 2H), 6.58 (ddd, $J = 7.3, 6.3, 1.2$ Hz, 2H), 5.48 (s, 2H), 3.77 (s, 3H), 3.76 (s, 6H); ^{13}C NMR (75 MHz, Acetone) δ 154.1 (2C), 152.1, 143.2, 139.2, 138.7, 137.8, 137.0, 125.7, 123.1 (2C), 121.1, 120.8, 119.9, 113.6, 111.2, 108.8, 106.9 (2C), 92.4, 60.6, 56.4 (2C); IR (cm^{-1}): 2928, 1587, 1500, 1412, 1343, 1235, 1125, 1005, 807. HRMS (ESI $^+$) for $\text{C}_{23}\text{H}_{22}\text{NO}_3$ [M + H] $^+$: calcd 360.1600 found 360.1613

4.2.4.6. *N*-Methyl-*N*-(2-methylquinolin-4-yl)pyrido[1,2-*a*]indol-2-amine **11b**

Protocol C. A sealed tube under argon atmosphere was charged at room temperature with 1 eq of **10b** and Pd/C (20 mol%) in *p*-xylene. The mixture was then heated at 145 °C for 48 h. Reaction completion was evaluated by analytical HPLC. The crude mixture was then allowed to cool down to room temperature, filtration through Celite, and the solvent was evaporated under reduced pressure. The crude product was purified by inverse phase column on preparative HPLC to give compounds 8 mg of **11b** as a brown solid (0.02 mmol, yield 32%); TLC (SiO_2 , 9/1 DCM/MeOH); $R_f = 0.65$; m.p. = 103 °C; ^1H NMR (300 MHz, Methanol- d_4) δ 8.66 – 8.45 (m, 2H), 8.12 (d, $J = 9.0$ Hz, 1H), 7.78 (d, $J = 8.4$ Hz,

1H), 7.66 – 7.52 (m, 2H), 7.45 (d, $J = 9.3$ Hz, 1H), 7.24 (d, $J = 8.6$ Hz, 1H), 7.18 – 7.13 (m, 1H), 7.12 (s, 1H), 7.01 (d, $J = 7.8$ Hz, 1H), 6.96 (d, $J = 9.5$ Hz, 1H), 6.58 (t, $J = 6.5$ Hz, 1H), 3.75 (s, 3H), 2.78 (s, 3H); ^{13}C NMR (75 MHz, Acetone- d_6) δ 164.0, 159.3, 155.8, 148.8, 147.1, 129.9, 128.2, 126.2, 125.7, 124.9, 123.3, 122.3, 119.6, 117.1, 116.2, 115.2, 113.9, 112.8, 111.8, 108.8, 92.2, 44.3, 24.4; IR (cm^{-1}): 2960, 2926, 1563, 1506, 1466, 1344, 1261, 1096, 800; HRMS (ESI $^+$) for $\text{C}_{23}\text{H}_{20}\text{N}_3$ [$\text{M} + \text{H}$] $^+$: calcd 338.1652 found 338.1693.

4.2.4.7. *N*-Methyl-*N*-(2-methylquinazolin-4-yl)pyrido[1,2-*a*]indol-2-amine **11c**

Protocol A followed by a *N*-methylation reaction and an oxidation step (Protocol C). A sealed tube under argon atmosphere was charged at room temperature with 1 eq of corresponding **9**, 1.2 eq of 2-methylquinazolin-4-amine (0.24 mmol), $\text{Pd}_2\text{dba}_3\cdot\text{CHCl}_3$ (5 mol%), XPhos (10 mol%) and 1.5 eqs (0.3 mmol) of NaOtBu in dry dioxane. The mixture was then heated at 100 °C for 1 h. The crude mixture was then allowed to cool down to room temperature, filtration through Celite with ethyl acetate, and the solvents were evaporated under reduced pressure. The crude residue was dissolved in freshly distilled DMF (4mL) at 0 °C and 2 eq of NaH were added. After 20 min., 1.2 eq of MeI was slowly added and the mixture was stirred at room temperature for 3 h. Reaction completion was evaluated by silica TLC (9/1 DCM/MeOH). The reaction was cooled to 0°C, saturated aqueous NH_4Cl solution was added by small portions and the mixture was extracted with EtOAc. The organic layer was washed with saturated aqueous NH_4Cl solution (2x), saturated aqueous NaHCO_3 solution (1x) and brine (2x). The combined organic layers were dried over MgSO_4 and concentrated in vacuum. The crude was charged under argon at room temperature with Pd/C (20 mol%) in *p*-xylene. The mixture was then heated at 145°C for 72 h. Reaction completion was evaluated by analytical HPLC. The crude mixture was then allowed to cool down to room temperature, filtration through a silica pad, and the solvent was evaporated under reduced pressure. The crude product was purified by inverse phase column on preparative to give 10mg of the product as red oil (0.03 mmol, yield 50%); TLC (SiO_2 , 95/5 DCM/MeOH); $R_f = 0.70$; ^1H NMR (200 MHz, CDCl_3) δ 8.31 (d, $J = 6.7$ Hz, 1H), 7.88 (d, $J = 8.9$ Hz, 1H), 7.77 (d, $J = 7.9$ Hz, 1H), 7.62 (s, 1H), 7.47 (t, $J = 9.1$ Hz, 2H), 7.09 (d, $J = 8.5$ Hz, 1H), 7.02 – 6.86 (m, 2H), 6.82 (d, $J = 7.0$ Hz, 1H), 6.58 (d, $J = 4.8$ Hz, 1H), 6.52 (d, $J = 6.4$ Hz, 1H), 3.74 (s, 3H), 2.77 (s, 3H); ^{13}C NMR (101 MHz, DMSO) δ 162.4, 161.3, 151.7, 143.4, 137.1, 131.7, 129.2, 127.4, 125.8, 125.6, 123.8, 123.0, 121.1, 118.7, 117.8, 116.6, 114.4, 113.0, 108.3, 91.4, 42.8, 26.1; IR (cm^{-1}): 3418, 3049, 2254, 1659, 1341, 1023, 1001, 890; HRMS (ESI $^+$) for $\text{C}_{22}\text{H}_{19}\text{N}_4$ [$\text{M} + \text{H}$] $^+$: calcd 339.1610 found 339.1613.

4.2.4.8. Synthesis of 8-bromo-3,4-dihydro-1H-[1,4]oxazino[4,3-*a*]indole **13**

1 eq (20 mg) of commercially available (5-bromo-1H-indol-2-yl)methanol **14a** was charged in a 25 mL round bottom flask, dissolved with 7 mL of fluorobenzene and cooled to 0 °C. Then, 3 eq (11mg) of NaH (60% dispersion in mineral oil) were slowly added to the solution. After 10 min. of stirring, the vinyl sulfonium salt was slowly injected to the solution. The reaction was next stirred at room temperature for 30 min. Evaporation of fluorobenzene gave a crude product which was purified by silica gel chromatography (95/5 to 85/15 cyclohexane/EtOAc). The product was then concentrated under vacuum to give 20.4 mg of **13** (91%) as a white solid.

4.2.4.9. 8-(1-(2-Methylquinolin-4-yl)vinyl)-3,4-dihydro-1H-[1,4]oxazino[4,3-*a*]indole **12a**

Protocol A. Column chromatography on silica gel afforded 50 mg of the product as a white-off solid (0.15 mmol, yield 82%); TLC (SiO_2 , 8/2 Cyclohexane/AcOEt); $R_f = 0.66$; m.p = 191°C; ^1H NMR (300 MHz, Acetone- d_6) δ 7.97 (d, $J = 8.5$ Hz, 1H), 7.70 (dd, $J = 8.4, 1.4$ Hz, 1H), 7.61 (ddd, $J = 8.4, 6.8, 1.5$ Hz, 1H), 7.36 (d, $J = 1.7$ Hz, 1H), 7.34 (s, 1H), 7.36 – 7.23 (m, 2H), 7.20 (dd, $J = 8.6, 1.8$ Hz, 1H), 6.11 (d, $J = 1.0$ Hz, 1H), 5.98 (d, $J = 1.4$ Hz, 1H), 5.31 (d, $J = 1.4$ Hz, 1H), 4.89 (d, $J = 1.2$ Hz, 2H), 4.14 (ddd, $J = 5.8, 4.2, 1.3$ Hz, 2H), 4.07 (ddd, $J = 6.0, 4.1, 1.3$ Hz, 2H), 2.72 (s, 3H); ^{13}C NMR (75 MHz, Acetone- d_6) δ 159.6, 150.0, 149.3, 148.8, 137.2, 135.3, 133.2, 130.0, 129.7, 129.1, 127.0, 126.3, 126.1, 123.1, 120.4, 119.5, 115.0, 109.8, 96.9, 65.2, 65.1, 42.6, 25.4; IR (cm^{-1}): 3052, 2958, 2924, 2358, 1592, 1481, 1371, 1107, 903, 768; HRMS (ESI $^+$) for $\text{C}_{23}\text{H}_{21}\text{N}_2\text{O}$ [$\text{M} + \text{H}$] $^+$: calcd 341.1654 found 341.1646.

4.2.4.10. 8-(1-(3,4,5-Trimethoxyphenyl)vinyl)-3,4-dihydro-1H-[1,4]oxazino[4,3-a]indole **12b**

Protocol A. Column chromatography on silica gel afforded 36mg of the product as a yellow solid (0.10 mmol, yield 62%); TLC (SiO₂, 7/3 Cyclohexane/EtOAc); R_f = 0.80; m.p = 131 °C; ¹H NMR (300 MHz, CDCl₃) δ 7.50 (s, 1H), 7.21 – 7.10 (m, 2H), 6.54 (s, 2H), 6.13 (s, 1H), 5.35 (d, *J* = 2.3 Hz, 1H), 5.29 (d, *J* = 2.4 Hz, 1H), 4.91 (s, 2H), 4.10 (dd, *J* = 6.4, 4.2 Hz, 2H), 4.02 (dd, *J* = 6.0, 4.4 Hz, 2H), 3.81 (s, 3H), 3.72 (s, 6H); ¹³C NMR (75 MHz, CDCl₃) δ 152.8 (2C), 151.1, 138.3, 137.8, 136.0, 133.6 (2C), 127.8, 121.9, 120.3, 112.5, 108.1, 105.9 (2C), 96.2, 65.0, 64.6, 60.9, 56.1 (2C), 41.9; IR (cm⁻¹): 2957, 2933, 1579, 1504, 1459, 1411, 1367, 1340, 1235, 1125, 1006; HRMS (ESI⁺) for C₂₂H₂₄NO₄ [M + H]⁺: calcd 366.1705 found 366.1696.

4.2.4.11. Methyl-N-(2-methylquinolin-4-yl)-3,4-dihydro-1H-[1,4]oxazino[4,3-a]indol-8-amine **12c**

Protocol B followed by a *N*-Methylation reaction. Column chromatography on silica gel afforded 43 mg of the product as a beige solid (0.12 mmol, yield 63%); TLC (SiO₂, 9/1 DCM/MeOH); R_f = 0.48; m.p = 190 °C; ¹H NMR (300 MHz, Methanol-*d*₄) δ 7.77 (dd, *J* = 8.3, 1.4 Hz, 1H), 7.53 – 7.35 (m, 2H), 7.25 (dd, *J* = 8.7, 1.7 Hz, 1H), 7.18 – 7.11 (m, 1H), 6.96 (s, 1H), 6.95 – 6.85 (m, 2H), 6.05 (s, 1H), 4.88 (s, 2H), 4.16 – 4.06 (m, 2H), 4.04 – 3.95 (m, 2H), 3.48 (s, 3H), 2.66 (s, 3H); ¹³C NMR (75 MHz, Methanol-*d*₄) δ 158.5, 155.1, 147.8, 143.8, 134.5, 134.0, 128.8, 128.7, 126.1, 125.6, 123.3, 120.7, 117.9, 115.3, 109.3, 108.4, 95.5, 64.2 (2C), 43.5, 41.5, 22.9; IR (cm⁻¹): 2924, 1585, 1480, 1415, 1337, 1092, 979, 765; HRMS (ESI⁺) for C₂₂H₂₂N₃O [M + H]⁺: calcd 344.1757 found 344.1758

4.2.4.12. *N*-Methyl-N-(3,4,5-trimethoxyphenyl)-3,4-dihydro-1H-[1,4]oxazino[4,3-a]indol-8-amine **12d**

Protocol B followed by a *N*-Methylation reaction. Column chromatography on silica gel afforded 20 mg of the product as a white off solid (0.10 mmol, yield 35%); TLC (SiO₂, 6/4 Cyclohexane/EtOAc); R_f = 0.63; m.p = 147 °C; ¹H NMR (300 MHz, Acetone-*d*₆) δ 7.34 (d, *J* = 8.7 Hz, 1H), 7.31 (d, *J* = 1.9 Hz, 1H), 6.96 (dd, *J* = 8.6, 2.0 Hz, 1H), 6.18 (s, 1H), 6.05 (s, 2H), 4.93 (s, 2H), 4.17 (dd, *J* = 5.8, 3.8 Hz, 2H), 4.13 – 4.06 (m, 2H), 3.66 (s, 6H), 3.64 (s, 3H), 3.28 (s, 3H); ¹³C NMR (75 MHz, Acetone-*d*₆) δ 154.5 (2C), 148.2, 143.3, 135.1 (2C), 134.8, 129.9, 120.3, 117.3, 110.3, 96.5, 95.1 (2C), 65.2 (2C), 60.6, 56.3 (2C), 42.6, 41.6; IR (cm⁻¹): 2933, 2837, 2825, 1604, 1583, 1508, 1240, 1173, 1008, 979; HRMS (ESI⁺) for C₂₁H₂₅N₂O₄ [M + H]⁺: calcd 369.1814 found 369.1817.

4.2.4.13. 4-((3,4-Dihydro-1H-[1,4]oxazino[4,3-a]indol-8-yl)(methyl)amino)quinoline-2-carbonitrile **12e**

Protocol B followed by a *N*-Methylation reaction. Column chromatography on silica gel afforded 20mg of the product as a yellow solid (0.05 mmol, yield 30%); TLC (SiO₂, 6/4 Cyclohexane/AcOEt); R_f = 0.46; m.p = 224 °C; ¹H NMR (300 MHz, Acetone-*d*₆) δ 7.92 (d, *J* = 8.5 Hz, 1H), 7.67 – 7.59 (m, 1H), 7.61 – 7.52 (m, 1H), 7.42 (s, 1H), 7.38 (d, *J* = 8.5 Hz, 1H), 7.28 (d, *J* = 2.3 Hz, 1H), 7.16 (ddd, *J* = 8.4, 6.7, 1.4 Hz, 1H), 7.02 (dd, *J* = 8.6, 2.3 Hz, 1H), 6.14 (s, 1H), 4.92 (d, *J* = 1.1 Hz, 2H), 4.24 – 4.15 (m, 2H), 4.15 – 4.08 (m, 2H), 3.59 (s, 3H); ¹³C NMR (75 MHz, CDCl₃) δ 155.0, 150.0 (2C), 143.6, 134.8, 134.3, 130.4, 129.9, 129.0, 126.7, 125.8, 123.0, 118.6, 116.2, 110.8, 110.1, 109.9, 96.3, 65.0, 64.6, 44.7, 42.0; IR (cm⁻¹): 2924, 2853, 2235, 1716, 1568, 1093, 800; HRMS (ESI⁺) for C₂₂H₁₉N₄O [M + H]⁺: calcd 355.1553 found 355.1558.

4.2.4.14. *N*-(2-Chloro-6,7-dimethoxyquinazolin-4-yl)-*N*-methyl-3,4-dihydro-1H-[1,4]oxazino[4,3-a]indol-8-amine **12f**

Protocol B followed by a *N*-Methylation reaction. Column chromatography on silica gel afforded 25 mg of the product as off-white solid (0.06 mmol, yield 37%); TLC (SiO₂, 5/5 Cyclohexane/AcOEt); R_f = 0.75; m.p = 218 °C; ¹H NMR (400 MHz, Acetone-*d*₆) δ 7.55 (dt, *J* = 8.6, 0.7 Hz, 1H), 7.51 (dd, *J* = 2.1, 0.6 Hz, 1H), 7.19 (dd, *J* = 8.5, 2.1 Hz, 1H), 6.98 (s, 1H), 6.26 (d, *J* = 1.0 Hz, 1H), 6.14 (s, 1H), 4.96 (d, *J* = 1.1 Hz, 2H), 4.24 – 4.13 (m, 4H), 3.88 (s, 3H), 3.61 (s, 3H), 2.88 (s, 3H); ¹³C NMR (101 MHz, Acetone) δ 162.3, 155.7, 155.2, 151.3, 148.1, 141.0, 136.6, 136.2, 130.0, 120.8, 119.3, 111.3, 109.4, 107.4, 106.7, 97.0, 65.1 (2C), 56.2, 55.0, 43.3, 42.8; IR (cm⁻¹): 2927, 1572, 1509, 1481, 1338, 1252, 1147, 957; HRMS (ESI⁺) for C₂₂H₂₂ClN₄O₃ [M + H]⁺: calcd 425.1380 found 425.1369.

4.2.4.15. *N*-Methyl-*N*-(2-methylquinazolin-4-yl)-3,4-dihydro-1*H*-[1,4]oxazino[4,3-*a*]indol-8-amine **12g**

Protocol B followed by a *N*-Methylation reaction. Column chromatography on silica gel afforded 35 mg of the product as a light brown solid (0.10 mmol, yield 35%); TLC (SiO₂, 8/2 Cyclohexane/EtOAc); R_f = 0.50; m.p = 191 °C; ¹H NMR (300 MHz, CD₂Cl₂) δ 7.65 (dd, *J* = 8.4, 1.4 Hz, 1H), 7.44 (ddd, *J* = 8.4, 6.8, 1.5 Hz, 1H), 7.36 (d, *J* = 2.1 Hz, 1H), 7.31 (dd, *J* = 8.6, 0.8 Hz, 1H), 7.01 (dd, *J* = 8.6, 2.1 Hz, 1H), 6.93 (dd, *J* = 8.6, 1.5 Hz, 1H), 6.80 (ddd, *J* = 8.4, 6.8, 1.4 Hz, 1H), 6.27 – 6.06 (m, 1H), 4.95 (d, *J* = 1.2 Hz, 2H), 4.16 (td, *J* = 4.7, 3.9, 1.5 Hz, 2H), 4.12 – 4.00 (m, 2H), 3.62 (s, 3H), 2.65 (s, 3H); ¹³C NMR (75 MHz, CD₂Cl₂) δ 163.7, 162.3, 152.6, 142.1, 135.5, 135.3, 131.9, 129.4, 127.9, 127.0, 124.0, 120.2, 118.3, 115.4, 110.4, 96.6, 65.3, 65.1, 43.6, 42.5, 26.7; IR (cm⁻¹): 2858, 1613, 1483, 1383, 1092, 766; HRMS (ESI⁺) for C₂₁H₂₁N₄O [M + H]⁺: calcd 345.1715 found 345.1716.

Bromoindole **14a** was *N*-alkylated as above (using 2 eq of NaH and 1.2 eq of EtI or MeI) and the crude product was then charged in a round bottom flask under argon with 1.1 eq of TBDMsCl and 1.1 eq of imidazole in dry DMF at room temperature overnight. A solution of saturated NH₄Cl was added by small portion and the mixture was extracted with EtOAc (3x). The organic layers were then washed twice with brine, dried over MgSO₄, concentrated in vacuum and purified by silica gel chromatography to give **14b** or **14c** as solids.

4.2.4.16. 5-Bromo-2-(((*tert*-butyldimethylsilyl)oxy)methyl)-1-ethyl-1*H*-indole **14b**

Column chromatography on silica gel afforded 715 mg of the product as a white solid (1.94 mmol, yield 97%); TLC (SiO₂, 7/3 Cyclohexane/EtOAc); R_f = 0.14; m.p = 76 °C; ¹H NMR (200 MHz, Chloroform-*d*) δ 7.70 (d, *J* = 1.8 Hz, 1H), 7.33 – 7.24 (m, 1H), 7.19 (d, *J* = 8.7 Hz, 1H), 6.32 (s, 1H), 4.82 (s, 2H), 4.24 (q, *J* = 7.2 Hz, 2H), 1.40 (t, *J* = 7.2 Hz, 3H), 0.92 (s, 9H), 0.09 (s, 6H); ¹³C NMR (75 MHz, CDCl₃) δ 139.6, 135.5, 129.2, 124.2, 123.2, 112.5, 110.6, 100.4, 58.0, 38.5, 25.9 (3C), 18.3, 15.3, -5.3 (2C); IR (cm⁻¹): 2954, 2929, 2857, 1471, 1446, 1412, 1140, 1051, 833, 779; HRMS (ESI⁺) for C₁₇H₂₇BrNOSi [M + H]⁺: calcd 368.1040 found 368.1040.

4.2.4.17. 5-Bromo-2-(((*tert*-butyldimethylsilyl)oxy)methyl)-1-methyl-1*H*-indole **14c**

Column chromatography on silica gel afforded 115 mg of the product as a white solid (1.13 mmol, yield 90%); TLC (SiO₂, 7/3 Cyclohexane/EtOAc); R_f = 0.13; m.p = 82 °C; ¹H NMR (300 MHz, Chloroform-*d*) δ 7.62 (d, *J* = 1.8 Hz, 1H), 7.21 (dd, *J* = 8.7, 1.9 Hz, 1H), 7.10 (d, *J* = 8.7 Hz, 1H), 6.25 (s, 1H), 4.75 (s, 2H), 3.69 (s, 3H), 0.84 (s, 9H), -0.00 (s, 6H); ¹³C NMR (75 MHz, CDCl₃) δ 140.2 (2C), 129.0, 124.3, 123.1, 112.5, 110.4, 100.2, 58.0, 30.1, 25.8 (3C), 18.2, -5.3 (2C); IR (cm⁻¹): 2948, 2925, 2853, 1462, 1388, 1248, 1142, 1052, 854; HRMS (ESI⁺) for C₁₆H₂₅BrNOSi [M + H]⁺: calcd 354.0883 found 354.0885.

Bromoindole **14a** was charged in a round bottom flask under argon with 2.5 eq of NaH in dry DMF at 0 °C for 30 min. Then, 3 eq of MeI were slowly injected and the mixture was stirred at room temperature for 2 h. At 0 °C a small quantity of water and a solution of saturated NH₄Cl were added by small portions before extraction with EtOAc (3x). The organic layers were then washed twice with brine and dried over MgSO₄. After concentration, the crude product was purified by silica gel chromatography (95/5 to 85/15 cyclohexane/EtOAc). Column chromatography on silica gel afforded 550 mg of the product as a pink pale solid (2.17 mmol, yield 87%); TLC (SiO₂, 6/4 Cyclohexane/EtOAc); R_f = 0.37; m.p = 77 °C; ¹H NMR (300 MHz, Methanol-*d*₄) δ 7.64 (d, *J* = 1.9 Hz, 1H), 7.28 (d, *J* = 8.7 Hz, 1H), 7.24 (dd, *J* = 8.7, 1.8 Hz, 1H), 6.42 (s, 1H), 4.61 (s, 2H), 3.74 (s, 3H), 3.35 (s, 3H); ¹³C NMR (75 MHz, MeOD) δ 138.7, 138.3, 135.5, 125.5, 123.9, 113.4, 111.9, 103.2, 67.2, 57.8, 30.2; IR (cm⁻¹): 2926, 1690, 1471, 1400, 1333, 1142, 1088, 866; HRMS (APCI) for C₁₁H₁₃BrNO [M + H]⁺: calcd 254.0181 found 254.0174.

4.2.4.18. 5-Bromo-2-((methoxymethoxy)methyl)-1-methyl-1*H*-indole **14e**

Bromoindole **14a** was *N*-methylated using 2 eq of NaH and 1.2 eq of MeI as above and the crude product was next charged in a round bottom flask under argon with 3 eq of DIPEA in dry DCM at room temperature for 20 min. Then, 2

eq of MOMCl were injected, and the reaction was stirred at 50 °C for 2 h. After completion, the reaction was neutralized with water, with 3 drops of HCl (1N) and was extracted with DCM. The combined organic layers were then washed twice with brine and were dried over MgSO₄. After concentration, the crude product was purified by silica gel chromatography (95/5 to 85/15 cyclohexane/EtOAc). Column chromatography on silica gel afforded 1067 mg of the product as a white solid (3.75 mmol, yield 91%); TLC (SiO₂, 7/3 Cyclohexane/EtOAc); R_f = 0.45; m.p = 65 °C; ¹H NMR (300 MHz, Acetone-*d*₆) δ 7.69 (d, *J* = 1.8 Hz, 1H), 7.35 (d, *J* = 8.7 Hz, 1H), 7.26 (dd, *J* = 8.7, 1.9 Hz, 1H), 6.47 (s, 1H), 4.74 (s, 2H), 4.67 (s, 2H), 3.80 (s, 3H), 3.37 (s, 3H); ¹³C NMR (75 MHz, Acetone) δ 138.8, 137.7, 130.0, 124.9, 123.6, 112.9, 112.0, 102.7, 96.0, 61.4, 55.5, 30.3; IR (cm⁻¹): 2941, 2849, 1470, 1399, 1332, 1146, 1097, 1027, 912, 865, 787; HRMS (APCI) for C₁₂H₁₅BrNO₂ [M + H]⁺: calcd 284.0286 found 284.0281.

4.2.4.19. (1-Ethyl-5-(1-(2-methylquinolin-4-yl)vinyl)-1H-indol-2-yl)methanol **15a**

Protocol A followed by a desilylation reaction. Column chromatography on silica gel afforded 30 mg of the product as a white-off solid (0.09 mmol, yield 65%) TLC (SiO₂, 6/4 cyclohexane/EtOAc); R_f = 0.84; m.p. = 182 °C; ¹H NMR (300 MHz, CD₂Cl₂) δ 7.97 (d, *J* = 8.5 Hz, 1H), 7.75 (d, *J* = 7.9 Hz, 1H), 7.58 (ddd, *J* = 8.3, 6.7, 1.4 Hz, 1H), 7.37 (s, 1H), 7.34 – 7.23 (m, 4H), 6.29 (s, 1H), 6.11 – 5.89 (m, 1H), 5.33 (br s, 1H), 4.76 (s, 2H), 4.26 (q, *J* = 7.2 Hz, 2H), 2.73 (s, 3H), 1.39 (t, *J* = 7.2 Hz, 3H); ¹³C NMR (75 MHz, CD₂Cl₂) δ 159.5, 149.9, 148.8, 148.0, 140.1, 137.4, 132.3, 129.5, 129.3, 128.1, 126.8, 126.2, 125.8, 123.1, 121.1, 120.0, 115.0, 110.0, 102.2, 57.8, 39.1, 25.6, 15.9; IR (cm⁻¹): 3247, 2958, 2924, 2854, 1593, 1482, 1378, 1260, 1081, 1013, 797; HRMS (ESI⁺) for C₂₃H₂₃N₂O [M + H]⁺: calcd 343.1805 found 343.1809.

4.2.4.20. (1-Ethyl-5-(1-(3,4,5-trimethoxyphenyl)vinyl)-1H-indol-2-yl)methanol **15b**

Protocol A followed by a desilylation reaction. Column chromatography on silica gel afforded 40 mg of the product as a orange yellow solid (0.11 mmol, yield 50%); TLC (SiO₂, 7/3 Cyclohexane/AcOEt); R_f = 0.90; m.p = 53 °C; ¹H NMR (400 MHz, Acetone-*d*₆) δ 7.49 (dd, *J* = 1.7, 0.7 Hz, 1H), 7.38 (dt, *J* = 8.5, 0.8 Hz, 1H), 7.17 (dd, *J* = 8.5, 1.8 Hz, 1H), 6.65 (s, 2H), 6.37 (d, *J* = 0.7 Hz, 1H), 5.38 (d, *J* = 1.6 Hz, 1H), 5.35 (d, *J* = 1.6 Hz, 1H), 4.78 (s, 2H), 4.34 (q, *J* = 7.1 Hz, 2H), 3.76 (s, 9H), 1.40 (t, *J* = 7.2 Hz, 3H); ¹³C NMR (101 MHz, Acetone-*d*₆) δ 154.0 (2C), 152.4, 141.2, 139.2, 139.1, 137.7, 133.4, 128.6, 122.8, 121.2, 112.3, 109.8, 107.1(2C), 101.9, 60.6, 57.3, 56.5(2C), 39.0, 15.8; IR (cm⁻¹): 3447, 2934, 1579, 1504, 1462, 1372, 1261, 1166, 1076; HRMS (ESI⁺) for C₂₂H₂₆NO₄ [M + H]⁺: calcd 368.1856 found 368.1863.

4.2.4.21. (1-Ethyl-5-(methyl(2-methylquinolin-4-yl)amino)-1H-indol-2-yl)methanol **15c**

Protocol B followed by a *N*-Methylation reaction and a desilylation step. Column chromatography on silica gel afforded 55 mg of the product as a yellow solid (0.16 mmol, yield 50%); TLC (SiO₂, 9/1 DCM/MeOH); R_f = 0.76; m.p = 177 °C; ¹H NMR (300 MHz, Chloroform-*d*) δ 7.98 (d, *J* = 8.4 Hz, 1H), 7.62 (d, *J* = 8.0 Hz, 1H), 7.50 (t, *J* = 7.6 Hz, 1H), 7.31 (d, *J* = 7.8 Hz, 1H), 7.27 (s, 1H), 7.09 (t, *J* = 7.5 Hz, 1H), 7.00 (dd, *J* = 8.7, 2.2 Hz, 1H), 6.92 (s, 1H), 6.34 (s, 1H), 4.84 (s, 2H), 4.31 (q, *J* = 7.2 Hz, 2H), 3.53 (s, 3H), 2.75 (s, 3H), 1.47 (t, *J* = 7.2 Hz, 3H); ¹³C NMR (75 MHz, CDCl₃) δ 159.0, 154.6, 143.7, 139.4, 134.1, 128.7, 128.3, 128.0, 125.3, 123.9, 121.6, 118.8, 114.9, 110.4, 110.3, 101.4, 57.2, 44.1, 38.5, 29.7, 25.2, 15.6; IR (cm⁻¹): 3241, 2924, 1585, 1480, 1414, 765; HRMS (ESI⁺) for C₂₂H₂₄N₃O [M + H]⁺: calcd 346.1914 found 346.1899.

4.2.4.22. (1-Ethyl-5-(methyl(2-methylquinazolin-4-yl)amino)-1H-indol-2-yl)methanol **15d**

Protocol B followed by a *N*-Methylation reaction and a desilylation step. Column chromatography on silica gel afforded 40 mg of the product as a pale yellow solid (0.11 mmol, yield 33%); TLC (SiO₂, 95/5 DCM/MeOH); R_f = 0.74; m.p = 63 °C; ¹H NMR (300 MHz, CD₂Cl₂) δ 8.48 (s, 1H), 8.08 (br s, 1H), 7.89 (d, *J* = 8.2 Hz, 1H), 7.69 – 7.50 (m, 1H), 7.48 – 7.33 (m, 1H), 7.06 (d, *J* = 8.6 Hz, 1H), 6.89 (t, *J* = 7.8 Hz, 1H), 6.79 (d, *J* = 8.5 Hz, 1H), 6.42 (s, 1H), 4.81 (s, 2H),

4.32 (q, $J = 6.4$ Hz, 2H), 3.74 (s, 3H), 2.75 (s, 3H), 1.43 (t, $J = 7.0$ Hz, 3H); ^{13}C NMR (75 MHz, CD_2Cl_2) δ 166.6, 162.1, 146.2, 141.7, 138.9, 136.6, 133.8, 129.0, 127.5, 125.7, 123.3, 120.1, 118.6, 114.0, 111.7, 102.1, 57.5, 44.6, 39.3, 24.1, 15.8; IR (cm^{-1}): 3246, 1584, 1566, 1498, 1482, 1385, 1348, 766; HRMS (ESI⁺) for $\text{C}_{21}\text{H}_{23}\text{N}_4\text{O}$ [$\text{M} + \text{H}$]⁺: calcd 347.1872 found 347.1876.

4.2.4.23. (1-Ethyl-5-(methyl(3,4,5-trimethoxyphenyl)amino)-1H-indol-2-yl)methanol **15e**

Protocol B followed by a *N*-Methylation reaction and a desilylation step. Column chromatography on silica gel afforded 20 mg of the product as a brown solid (0.11 mmol, yield 13%); TLC (SiO_2 , 7/3 Cyclohexane/EtOAc); $R_f = 0.62$; m.p = 104 °C; ^1H NMR (300 MHz, Acetone- d_6) δ 7.35 (d, $J = 4.2$ Hz, 1H), 7.33 (d, $J = 2.5$ Hz, 1H), 7.05 (dd, $J = 8.8, 1.6$ Hz, 1H), 6.40 – 6.28 (m, 3H), 4.58 (s, 2H), 4.24 (q, $J = 7.1$ Hz, 2H), 3.72 (s, 6H), 3.65 (s, 3H), 3.32 (s, 3H), 1.35 (t, $J = 7.1$ Hz, 3H); ^{13}C NMR (75 MHz, Acetone- d_6) δ 155.7 (2C), 139.9, 137.0, 136.7, 129.1, 117.9, 117.6, 112.4, 110.7 (2C), 103.1, 94.3 (2C), 67.0, 60.7, 57.5, 56.2 (2C), 38.9, 15.7; IR (cm^{-1}): 3363, 2854, 2823, 1604, 1506, 1463, 1232, 1213, 1127, 1010; HRMS (ESI⁺) for $\text{C}_{21}\text{H}_{27}\text{N}_2\text{O}_4$ [$\text{M} + \text{H}$]⁺: calcd 371.1971 found 371.1992.

4.2.4.24. (1-Methyl-5-(1-(2-methylquinolin-4-yl)vinyl)-1H-indol-2-yl)methanol **15f**

Protocol A followed by a desilylation reaction. Column chromatography on silica gel afforded 26 mg of the product as a white-off solid (0.07 mmol, yield 40%) TLC (SiO_2 , 5/5 cyclohexane/EtOAc); $R_f = 0.83$; m.p. = 217 °C; ^1H NMR (300 MHz, DMSO- d_6) δ 7.95 (d, $J = 8.4$ Hz, 1H), 7.69 – 7.59 (m, 1H), 7.58 (d, $J = 8.3$ Hz, 1H), 7.37 (t, $J = 4.2$ Hz, 2H), 7.32 (d, $J = 8.1$ Hz, 1H), 7.28 (s, 1H), 7.17 (dd, $J = 8.6, 1.7$ Hz, 1H), 6.27 (s, 1H), 5.99 (s, 1H), 5.29 (s, 1H), 5.18 (t, $J = 5.2$ Hz, 1H), 4.59 (d, $J = 4.8$ Hz, 2H), 3.71 (s, 3H), 2.71 (s, 3H); ^{13}C NMR (75 MHz, DMSO) δ 158.6, 148.7, 147.6, 146.8, 141.4, 137.3, 130.8, 129.0, 128.6, 126.9, 125.7, 125.4, 124.9, 122.2, 119.6, 118.3, 114.6, 109.6, 100.4, 55.4, 29.7, 24.8. IR (cm^{-1}): 3252, 2941, 2924, 1595, 1488, 1378, 1072, 1022; HRMS (ESI⁺) for $\text{C}_{22}\text{H}_{21}\text{N}_2\text{O}$ [$\text{M} + \text{H}$]⁺: calcd 329.1648 found 329.1651.

4.2.4.25. (1-Methyl-5-(1-(3,4,5-trimethoxyphenyl)vinyl)-1H-indol-2-yl)methanol **15g**

Protocol A followed by a desilylation reaction. Column chromatography on silica gel afforded 15 mg of the product as a brown pale oil (0.04 mmol, yield 50%); TLC (SiO_2 , 5/5 Cyclohexane/AcOEt); $R_f = 0.55$; ^1H NMR (300 MHz, Acetone- d_6) δ 7.49 (d, $J = 1.8$ Hz, 1H), 7.34 (d, $J = 8.6$ Hz, 1H), 7.17 (dd, $J = 8.5, 1.7$ Hz, 1H), 6.64 (s, 2H), 6.39 (s, 1H), 5.37 (d, $J = 2.0$ Hz, 2H), 4.78 (d, $J = 5.5$ Hz, 2H), 4.16 (t, $J = 5.6$ Hz, 1H), 3.83 (s, 3H), 3.78 – 3.73 (m, 9H); ^{13}C NMR (75 MHz, Acetone- d_6) δ 154.0 (2C), 152.3, 141.8, 139.2, 139.0, 138.8, 133.4, 128.3, 122.8, 121.1, 112.2, 109.6, 107.0 (2C), 101.6, 60.6, 57.2, 56.4 (2C), 27.5; IR (cm^{-1}): 3435, 2933, 1579, 1412, 1345, 1236, 1125, 1005; HRMS (ESI⁺) for $\text{C}_{21}\text{H}_{24}\text{NO}_4$ [$\text{M} + \text{H}$]⁺: calcd 354.1700 found 354.1700.

4.2.4.26. (1-Methyl-5-(methyl(2-methylquinolin-4-yl)amino)-1H-indol-2-yl)methanol **15h**

Protocol B followed by a *N*-methylation reaction and a desilylation step. Column chromatography on silica gel afforded 20 mg of the product as a deep yellow solid (0.06 mmol, yield 45%); TLC (SiO_2 , 8/2 DCM/MeOH); $R_f = 0.33$; m.p = 192 °C; ^1H NMR (300 MHz, Methanol- d_4) δ 7.77 (d, $J = 9.0$ Hz, 1H), 7.48 – 7.37 (m, 2H), 7.31 (d, $J = 8.7$ Hz, 1H), 7.17 (d, $J = 2.2$ Hz, 1H), 7.03 – 6.93 (m, 2H), 6.92 – 6.86 (m, 1H), 6.30 (s, 1H), 4.71 (s, 2H), 3.77 (s, 3H), 3.50 (s, 3H), 2.67 (s, 3H); ^{13}C NMR (75 MHz, Methanol- d_4) δ 159.8, 156.6, 149.0, 144.6, 142.0, 137.3, 130.2, 129.5, 127.4, 127.2, 124.7, 122.0, 120.2, 117.1, 111.4, 109.6, 102.2, 57.2, 45.0, 30.2, 24.2; IR (cm^{-1}): 3226, 2962, 1637, 1507, 1428, 1014, 765; HRMS (ESI⁺) for $\text{C}_{21}\text{H}_{22}\text{N}_3\text{O}$ [$\text{M} + \text{H}$]⁺: calcd 332.1763 found 332.1758.

4.2.4.27. *N*-(2-((Methoxymethoxy)methyl)-1-methyl-1H-indol-5-yl)-*N*,2-dimethylquinolin-4-amine **15i**

Protocol B followed by a *N*-methylation reaction. Column chromatography on silica gel afforded 145 mg of the product as a yellow powder (0.39 mmol, yield 73%); TLC (SiO_2 , 9/1 DCM/MeOH); $R_f = 0.45$; m.p = 122 °C; ^1H NMR (300 MHz, MeOD) δ 7.77 (d, $J = 8.8$ Hz, 1H), 7.48 – 7.34 (m, 2H), 7.25 (d, $J = 8.7$ Hz, 1H), 7.14 (d, $J = 2.2$ Hz, 1H), 6.94

(s, 1H), 6.94 – 6.90 (m, 1H), 6.90 – 6.85 (m, 1H), 6.29 (s, 1H), 4.66 (s, 2H), 4.63 (s, 2H), 3.70 (s, 3H), 3.45 (s, 3H), 3.36 (s, 3H), 2.65 (s, 3H); ¹³C NMR (75 MHz, MeOD) δ 160.1, 156.5, 149.5, 144.8, 138.4, 137.2, 130.1, 129.3, 127.8, 127.1, 124.7, 122.2, 120.4, 117.0, 111.4, 110.0, 103.9, 96.2, 61.9, 55.8, 44.9, 30.2, 24.5; IR (cm⁻¹): 2940, 2828, 1578, 1480, 1083, 763, 731; HRMS (ESI⁺) for C₂₃H₂₆N₃O₂ [M + H]⁺: calcd 376.2025 found 376.2021.

4.2.4.28. *N*-(2-(Methoxymethyl)-1-methyl-1*H*-indol-5-yl)-*N*,2-dimethylquinolin-4-amine **15j**

Protocol B followed by a *N*-methylation reaction. Column chromatography on silica gel afforded 660 mg of the product as a yellow solid (1.74 mmol, yield 84%); TLC (SiO₂, 9/1 DCM/MeOH); R_f = 0.55; m.p = 156 °C; ¹H NMR (300 MHz, CDCl₃) δ 7.95 (d, *J* = 8.3 Hz, 1H), 7.55 (d, *J* = 8.5 Hz, 1H), 7.45 (t, *J* = 7.6 Hz, 1H), 7.26 – 7.15 (m, 2H), 7.02 (t, *J* = 7.7 Hz, 1H), 6.94 (dd, *J* = 8.7, 1.8 Hz, 1H), 6.87 (s, 1H), 6.35 (s, 1H), 4.55 (s, 2H), 3.73 (s, 3H), 3.48 (s, 3H), 3.35 (s, 3H), 2.72 (s, 3H); ¹³C NMR (75 MHz, CDCl₃) δ 158.9, 154.6, 149.0, 143.8, 136.8, 135.4, 128.7, 128.3, 127.7, 125.3, 123.9, 121.6, 118.9, 114.9, 110.3, 110.1, 102.9, 66.4, 57.5, 44.1, 29.9, 25.2; IR (cm⁻¹): 2924, 2881, 1585, 1481, 1083, 764, 731; HRMS (ESI⁺) for C₂₂H₂₄N₃O [M + H]⁺: calcd 346.1919 found 346.1910.

4.2.4.29. 2-(Methoxymethyl)-*N*,1-dimethyl-*N*-(3,4,5-trimethoxyphenyl)-1*H*-indol-5-amine **15k**

Protocol B followed by a *N*-methylation reaction. Column chromatography on silica gel afforded 160 mg of the product as a pale brown oil (0.43 mmol, yield 55%); TLC (SiO₂, 6/4 Cyclohexane/AcOEt); R_f = 0.55; ¹H NMR (300 MHz, Chloroform-*d*) δ 7.39 (d, *J* = 1.9 Hz, 1H), 7.28 (d, *J* = 8.7 Hz, 1H), 7.06 (dd, *J* = 8.7, 2.1 Hz, 1H), 6.45 (s, 1H), 6.02 (s, 2H), 4.60 (s, 2H), 3.79 (s, 3H), 3.78 (s, 3H), 3.73 (s, 6H), 3.38 (s, 3H), 3.32 (s, 3H); ¹³C NMR (75 MHz, CDCl₃) δ 153.4 (2C), 147.2, 141.7, 136.5, 135.8, 130.7, 127.9, 120.9, 117.1, 110.0, 102.9, 93.6 (2C), 66.5, 61.0, 57.5, 56.0 (2C), 41.4, 29.9; IR (cm⁻¹): 2930, 2581, 1506, 1485, 1236, 1124, 1082, 975, 729; HRMS (ESI⁺) for C₂₁H₂₇N₂O₄ [M + H]⁺: calcd 371.1971 found 371.1959.

4.2.4.30. 2-(Methoxymethyl)-1-methyl-5-(1-(3,4,5-trimethoxyphenyl)vinyl)-1*H*-indole **15l**

Protocol A. Column chromatography on silica gel afforded 115 mg of the product as a pale yellow solid (0.31 mmol, yield 80%); TLC (SiO₂, 7/3 Cyclohexane/EtOAc); R_f = 0.59; m.p = 123 °C; ¹H NMR (300 MHz, Acetone-*d*₆) δ 7.52 (dd, *J* = 1.7, 0.7 Hz, 1H), 7.36 (dd, *J* = 8.6, 0.8 Hz, 1H), 7.19 (dd, *J* = 8.6, 1.7 Hz, 1H), 6.65 (s, 2H), 6.47 (s, 1H), 5.44 – 5.32 (m, 2H), 4.61 (s, 2H), 3.79 (s, 3H), 3.76 (s, 3H), 3.76 (s, 6H), 3.34 (s, 3H); ¹³C NMR (75 MHz, Acetone-*d*₆) δ 154.0 (2C), 152.3, 139.2, 139.0 (2C), 138.9, 138.0, 133.6, 128.1, 123.1, 121.2, 112.4, 109.7, 107.0 (2C), 103.6, 66.9, 60.6, 57.5, 56.4 (2C); IR (cm⁻¹): 2935, 2828, 2358, 1578, 1503, 1450, 1410, 1365, 1235, 1174, 1084; HRMS (ESI⁺) for C₂₂H₂₆NO₄ [M + H]⁺: calcd 368.1862 found 368.1878.

4.3. Biology

4.3.1. Cell Culture and Proliferation Assay

Cancer cell lines were obtained from the American type Culture Collection (Rockville, MD) and were cultured according to the supplier's instructions. K562R (doxorubicin-resistant) leukemia cells were a generous gift from JP Marie (France). Briefly, human HCT-116 colorectal carcinoma cells were grown in Gibco McCoy's 5A supplemented with 10% fetal calf serum and 1% glutamine. A549 lung carcinoma, MDA-MB231 breast carcinoma, K562 and K562R leukemia cells were grown in RPMI 1640 supplemented with 10% fetal calf serum and 1% glutamine. U87-MG glioblastoma, Mia Paca-2 pancreatic carcinoma and HT29 colorectal carcinoma cells were grown in Dulbecco minimal essential medium (DMEM) containing 4.5 g/L glucose supplemented with 10% FCS and 1% glutamine. All cell lines were maintained at 37 °C in a humidified atmosphere containing 5% CO₂. Cell viability was determined by a luminescent assay according to the manufacturer's instructions (Promega, Madison, WI, USA). For IC₅₀ determination, the cells were seeded in 96-well plates (3 × 10³ cells/well) containing 90 μL of growth medium. After 24 h of culture, the cells were treated with the tested compounds at 10 different final concentrations. Each concentration was obtained from serial dilutions in culture medium starting from the stock solution. Control cells were treated with the vehicle.

Experiments were performed in triplicate. After 72 h of incubation, 100 μ L of CellTiter Glo Reagent was added for 15 min before recording luminescence with a spectrophotometric plate reader PolarStar Omega (BMG LabTech). The dose-response curves were plotted with Graph Prism software and the IC₅₀ values were calculated using the Graph Prism software from polynomial curves (four or five-parameter logistic equations).

4.3.2. Metabolization study of **15b** and **15d**

4.3.2.1 Chemicals

The two synthesized **15b** and **15d** were characterized by NMR spectroscopy and HRMS spectrometry with a HPLC-UV purity of >99%.

Glucose-6-phosphate, glucose-6-phosphate dehydrogenase and nicotinamide adenine dinucleotide phosphate tetra sodium (NADPNa₄) were provided by Sigma-Aldrich (St Louis, MO, USA). LC/MS-grade acetonitrile, LC/MS-grade water, methanol and formic acid were purchased from Merck (Darmstadt, Germany). Stock solutions of the two compounds were prepared at 1600 μ g/mL (about 4 mM) in methanol/dichloromethane (96/4, v:v) and stored at 4°C until the *in vitro* metabolism study.

4.3.2.2 High performance liquid chromatography-mass spectrometry (HPLC-MS)

HPLC-MS chromatograms were performed using an Alliance 2695 HPLC system (Waters, Milford, USA) fitted with a XBridge C18 column (2.1 \times 150 mm, 3.5 μ m). Gradient elution was achieved with a flow rate of 0.25 mL/min using water with 0.1% formic acid (solvent A) and acetonitrile with 0.1% formic acid (solvent B) from A:B (95/5, v:v) to A:B (0/100, v:v) in 20 min. Analytes were detected with a LCT[®] Premier time-of-flight mass spectrometer (Waters, Milford, USA) operating in positive electrospray ionization mode scanning from 100 to 1000 m/z with 10 spectra/s. MS parameters settings were: capillary and cone voltage at 3500 V and 25 V. High resolution mass spectra (HRMS) were processed using MassLynx[®] software.

4.3.2.3 High performance liquid chromatography-tandem mass spectrometry (HPLC-MS/MS)

HPLC-MS/MS analyses were performed using a HPLC system (Ultimate 3000, Dionex, USA) fitted with a Hypersil[®] C18 column (2.1 \times 100 mm, 5 μ m) Thermo Fischer Scientific Inc, Waltham, MA, USA. Isocratic elution was achieved with a flow rate of 200 μ L/min of the mobile phase, acetonitrile/water (60:40, v/v) with 0.2% formic acid. The total run time was 5 min. After injection of 10 μ L, HPLC-MS/MS analyses were performed using the LTQ-Orbitrap[™] Velos Pro hybrid mass spectrometer (Thermo Fischer Scientific Inc, Waltham, MA, USA), controlled by the Xcalibur[®] software operating in positive electrospray ionization at unit mass resolution by scanning over m/z 150 to 450 using collision-induced dissociation of the selected precursor ions. Quantification of compounds was performed by selective reaction monitoring with the following ion transitions: m/z 347.1 \rightarrow 332.1 for **15d**, m/z 368.1 \rightarrow 338.1 for **15b** and m/z 317.1 \rightarrow 302.1 for IS (*isoCA-4*). Collision energy was optimized at 45 eV for **15d** and at 25 eV for **15b** and *isoCA-4* using helium as collision gas. HPLC-MS/MS analyses were processed using Xcalibur[®] software. Calibration curves of each compound were fitted with 1/ c weighted least-squares regression by plotting the peak area ratio of each analyte to IS against the analyte concentration over the calibration range (1-50 μ g/mL or 3-140 nM/mL) in buffer (PH 7.4). The ESI-MS parameters were set as follows: spray voltage at 3400 V, source heater and capillary temperature at 300 °C and 350 °C, respectively with drying gas flowrate at 40 L/h.

4.3.2.4 Incubation of CH compounds with rat and human liver microsomes

Rat liver microsomes (RLM) and human liver microsomes (HLM) were provided at a protein concentration of 20 mg/mL by Thermofischer Scientific Inc, Waltham, MA, USA. Incubations were performed at a final protein concentration of 1 mg/mL for microsomal suspensions in 10 mM buffer (pH 7.4). After pre-warming at 37 °C, in the

presence of a NADPH-generating system consisting in 0.6 mM NADPNa₄, 6.4 mM glucose-6-phosphate and 2 U/mL glucose-6-phosphate dehydrogenase, the incubation started by the addition of substrate at a final 100 μM concentration (2% of total incubation volume) and the solution was shaken at 37 °C. After the incubation time of 0, 1, 3, 6, 24, 48, 72, 96 h (up to 144 h), 50 μL aliquots (in triplicate) were drawn in polypropylene tubes containing 100 μL of internal standard solution (*iso*CA-4, 2500 ng/mL acetonitrile) and mixed with 1 mL of ethyl acetate to stop the reaction. After centrifugation at 13,000 rpm for 4 min. and evaporation of the recovered organic phase under vacuum centrifugation at 40 °C, the residue was dissolved in 0.1 mL of acetonitrile and analysed by HPLC-MS/MS.

4.3.3. Tubulin Binding Assay

Porcine brain tubulin was isolated following Shelanski procedure.[41] Tubulin was solved in 0.1 M MES buffer, 1.5 mM GTP, 1 mM EGTA, 1 mM β-ME, 1 mM MgCl₂, pH 6.7 buffer and centrifuged at 50000 rpm for 30 min in a TLA-100.3 rotor (Beckman Optima TLX centrifuge). Tubulin was then diluted to 1.5 mg/mL. Samples, containing the ligand or DMSO (negative control), were incubated 30 min at 20 °C, followed by cooling on ice for 10 min. Tubulin polymerization was assessed by the UV absorbance increase at 450 nm (in Helios Alpha spectrophotometer, Thermo Fisher Scientific) due to the turbidity caused by a temperature shift from 4 °C to 37 °C. When a stable absorbance value was reached and maintained for at least 20 min, the temperature was switched back to 4 °C to ascertain the return to the initial absorption values, to confirm the reversibility of the process. The degree of tubulin assembly for each experiment was calculated as the difference in amplitude between the stable plateau (absorbance at 37 °C) and the initial baseline of the curves (absorbance at 4 °C). Control experiments in identical conditions but with the absence of ligand were taken as 100% tubulin polymerization. The IC₅₀ value of tubulin polymerization was determined by measuring the tubulin polymerization inhibitory activity at different ligand concentrations. The obtained values of the mole ratio of total ligand to total tubulin in solution were fitted to mono exponential curves and the IC₅₀ values of tubulin polymerization inhibition were calculated from the best-fitting curve of three independent experiments using Graphpad Prism 7.0 software.

4.3.4. Cell Cycle Analysis

Exponentially growing cancer K562 were incubated with **15d** at different concentrations (0.5 and 1 nM) or in DMSO alone for 24 h. Cell-cycle profiles were determined by flow cytometry on a FC500 flow cytometer (Beckman-Coulter, France) as described previously.[49]

4.3.5. Mitochondrial membrane potential assay

One of the hallmark for apoptosis is the loss of mitochondrial membrane potential ($\Delta\Psi_m$). The changes in the mitochondrial potential were detected by 5,5',6,6'-tetrachloro-1,1',3,3'-tetraethylbenzimidazolylcarbocyanine iodide/chloride (JC-1), a cationic dye that exhibits potential dependent accumulation in mitochondria, indicated by fluorescence emission shift from red (590 nm) to green (525 nm). In brief, K562 cells were treated with different concentrations of indole **15d** for 48 h. After treatment, cells were re-suspended in 1 mL of PBS containing 2 μM final concentration JC-1 probe and incubated at 37 °C for 15 min. Analysis of cells was performed on a FC500 flow cytometer (Beckman Coulter, France).

4.4. Colony Formation Assays

For colony formation assays, human chronic myeloid leukemia K562 cells (ATCC, CCL-243, Manassas, VA, USA) were cultured in Roswell Park Memorial Institute (RPMI) 1640 medium (Lonza, Basel, Switzerland), supplemented with 10% heat-inactivated fetal bovine serum (FBS) (Biowest, Riverside, CA, USA) and 1% penicillin-streptomycin solution (100×) (GenDEPOT, Katy, TX, USA). Imatinib-resistant K562 (K562IR) cells were a gift of the Catholic University of Seoul, South Korea and cultured in RPMI 1640 medium with 25 mM HEPES (Lonza) supplemented with 10% (v/v) FCS and 1% (v/v) antibiotic-antimycotics. K562IR cells were cultured with 1 μM of imatinib and washed three times before each experiment. Cells were maintained at 37 °C and 5% of CO₂ in a humidified atmosphere. Mycoplasma detection by MycoalertTM (Lonza) was performed every 30 days, and cells were used within three months

after thawing. For the colony formation assay, 10^3 K562 or K562IR cells were counted and grown in a semisolid methylcellulose medium (Methocult H4230, StemCell Technologies Inc., Vancouver, BC, Canada) supplemented with 10% FBS in absence or presence of indicated concentrations of **15d**. Colonies were detected after 10 days of culture by adding 1mg/mL of 3-(4,5-dimethylthiazol-2-yl)-2,5-diphenyltetrazolium bromide (MTT) reagent (Sigma-Aldrich) and were analyzed by Image J 1.8.0 software (U.S. National Institute of Health, Bethesda, MD, USA). Data of three independent experiments are expressed as the mean \pm SD and significance was estimated by using two-way ANOVA (analysis of variance) followed by Tukey's multiple comparison test, unless otherwise stated, using GraphPad Prism 8 Software (La Jolla, CA, USA). *p*-values were considered statistically significant when $p < 0.05$. Legends are represented as follows: * $p < 0.05$, ** $p < 0.01$, *** $p < 0.001$.

4.5. Molecular modeling

Atomic coordinates for tubulin α,β -dimer were retrieved from the Protein Data Bank (accession code 6H9B). Missing hydrogen atoms were added using the Dock Prep module from the UCSF Chimera v1.13 software package [50], and atoms from the ligand co-crystallized in the colchicine binding at the interface between chains C and D were deleted. Coordinates for a low-energy starting conformer of compound **15d** were obtained using the Conformers function from MarvinSketch v19.12 software package [51] with default parameters. Molecular docking was performed using AutoDock Vina v1.1.2 software package [52] with default parameters and the binding site defined as the box circumscribed to all the protein residues in contact with the co-crystallized ligand. Analysis and depiction of poses were performed using UCSF Chimera v1.13 software package [50].

Acknowledgments

The authors gratefully acknowledge support of this project by CNRS and University Paris-Saclay. S. Pecnard thank La Ligue contre le Cancer for its Ph.D. funding. L. Gallego-Yerga and R. Peláez acknowledge the support by the Spanish Ministry of Science, Innovation and Universities (RTI2018-099474-BI00), co-funded by the EU's European Regional Development Fund FEDER. Ji Yeon Paik and Marc Diederich thank the National Research Foundation (NRF) of Korea [Grant Number 019R1A2C1009231], the Brain Korea (BK21) FOUR program and the Creative-Pioneering Researchers Program at Seoul National University [Funding number: 370C-20160062]. Marc Diederich thanks the "Recherche Cancer et Sang" Foundation, "Recherches Scientifiques Luxembourg", "Een Häerz fir kriibskrank Kanner", Action Lions "Vaincre le Cancer", and Télévie Luxembourg.

References

- [1] G. R. Pettit, S. B. Singh, E. Hamel, C. M. Lin, D. S. Alberts, D. Garcia-Kendall, Isolation and structure of the strong cell growth and tubulin inhibitor combretastatin A-4, *Experientia* 45 (1989) 209-211.
- [2] A. T. Mc Gown, B. W. Fox, Differential cytotoxicity of combretastatins A1 and A4 in two daunorubicin-resistant P388 cell lines, *Cancer Chemother. Pharmacol.* 26 (1990) 79-81.
- [3] C. M. Lin, H. H. Ho, G. R. Pettit, E. Hamel, Antimitotic natural products combretastatin A-4 and combretastatin A-2: studies on the mechanism of their inhibition of the binding of colchicine to tubulin, *Biochemistry* 28 (1989) 6984-6991.
- [4] G.G. Dark, S.A. Hill, V.E. Prise, G.M. Tozer, G.R. Pettit, D.J. Chaplin. Combretastatin A-4, an agent that displays potent and selective toxicity toward tumor vasculature. *Cancer Res.* 57 (1997) 1829-1834.
- [5] G. M. Tozer, V. E. Prise, J. Wilson, R. J. Locke, B. Vojnovic, M. R. Stratford, M. F. Dennis, D. J. Chaplin, Combretastatin A-4 phosphate as a tumor vascular-targeting agent: Early effects in tumors and normal tissues, *Cancer Res.* 59 (1999) 1626-1634.
- [6] G. M. Tozer, C. Kanthou, C. S. Parkins, S. A. Hill, The biology of the combretastatins as tumour vascular targeting agents, *Int. J. Exp. Pathol.* 83 (2002) 21-38.
- [7] Z.S. Seddigi, M.M. Shaheer, S.A. Prasanth, A.S.A. Babalghith, A.O. Lamfon, H.A. Kamal, A. Recent advances in combretastatin based derivatives and prodrugs as antimitotic agents. *MedChemComm* 8 (2017) 1592-1603.
- [8] A. Siebert, M. Gensicka, G. Cholewinski, K. Dzierzbicka. Synthesis of Combretastatin A-4 Analogs and their Biological Activities *Anti-Cancer Agents in Medicinal Chemistry* 18 (2016) 942-960.

- [9] Y. Shan, J. Zhang, Z. Liu, M. Wang, Y. Dong. Developments of combretastatin A-4 derivatives as anticancer agents. *Curr. Med. Chem.* 18 (2011) 523-538.
- [10] K. Ohsumi, T. Hatanaka, R. Fujita, R. Nakagawa, Y. Fukuda, Y. Nihei, Y. Suga, Y. Morinaga, Y. Akiyama, T. Tsuji, Syntheses and antitumor activity of cis-restricted combretastatins: 5-membered heterocyclic analogues, *Bioorg. Med. Chem. Lett.* 8 (1998) 3153-3158.
- [11] S. Aprile, E. Del Grosso, G. C. Tron, G. Grosa, Identification of the Human UDP-Glucuronosyltransferases Involved in the Glucuronidation of Combretastatin A-4, *Drug Metab. Dispos.* 35 (2007) 2252-2261.
- [12] C.-H. Shen, J.-J. Shee, J.-Y. Wu, Y.-W. Lin, J.-D. Wu, Y.-W. Liu, Combretastatin A-4 inhibits cell growth and metastasis in bladder cancer cells and retards tumour growth in a murine orthotopic bladder tumour model. *Br. J. Pharmacol.* 160 (2010) 2008-2027.
- [13] O. Provot, A. Hamze, J. F. Peyrat, J. D. Brion, M. Alami, Discovery and Hit to Lead Optimization of Novel Combretastatin A-4 Analogues: Dependence of C-Linker Length and Hybridization, *Anti-Cancer Agents Med. Chem.* 13 (2013) 1614-1635.
- [14] S. Messaoudi, B. Tréguier, A. Hamze, O. Provot, J. F. Peyrat, J. R. Rodrigo De Losada, J. M. Liu, J. Bignon, J. Wdzieczak-Bakala, S. Thoret, J. Dubois, J. D. Brion, M. Alami, Isocombretastatins A versus Combretastatins A: The Forgotten *isoCA-4* Isomer as a Highly Promising Cytotoxic and Antitubulin Agent, *J. Med. Chem.* 52 (2009) 4538-4542.
- [15] R. Alvarez, C. Alvarez, F. Mollinedo, B.G. Sierra, M. Medarde, R. Pelaez, Isocombretastatins A: 1, 1-diarylethenes as potent inhibitors of tubulin polymerization and cytotoxic compounds, *Bioorg. Med. Chem.* 17 (2009), 6422-6431.
- [16] A. Hamze, A. Giraud, S. Messaoudi, O. Provot, J. F. Peyrat, J. Bignon, J. M. Liu, J. Wdzieczak-Bakala, S. Thoret, J. Dubois, J. D. Brion, M. Alami, Synthesis, Biological Evaluation of 1,1-Diarylethylenes as a Novel Class of Antimitotic Agents, *ChemMedChem* 4 (2009) 1912-1924.
- [17] M.A. Soussi, S. Aprile, S. Messaoudi, O. Provot, E. Del Grosso, J. Bignon, J. Dubois, J.D. Brion, G. Grosa, M. Alami. Metabolites of *isoCombretastatin A-4* in Human Liver Microsomes: Identification, Synthesis and Biological Evaluation, *ChemMedChem* 6 (2011) 1781-1788.
- [18] A. Hamze, E. Rasolofonjatovo, O. Provot, C. Mousset, D. Veau, J. Rodrigo, J. Bignon, J. M; Liu, J. Wdzieczak-Bakala, S. Thoret, J. Dubois, J. D. Brion, M. Alami, B-Ring-Modified *isoCombretastatin A-4* Analogues Endowed with Interesting Anticancer Activities, *ChemMedChem* 6 (2011) 2179-2191.
- [19] For a review on *isoCA-4* analogues see: M. Alami, A. Hamze, O. Provot, Developments of *isoCombretastatin A-4* Derivatives as Highly Cytotoxic Agents. *Eur. J. Med. Chem.* (2020), 112110.
- [20] S. Messaoudi, A. Hamze, O. Provot, B. Tréguier, J. Rodrigo De Losada, J. Bignon, J.-M. Liu, J. Wdzieczak-Bakala, S. Thoret, J. Dubois, J.D. Brion, M. Alami, Discovery of Novel *isoErianin* Analogues as Promising Anticancer Agents, *ChemMedChem* 6 (2011) 488-497.
- [21] E. Rasolofonjatovo, O. Provot, A. Hamze, J. Rodrigo, J. Bignon, J. Wdzieczak-Bakala, D. Desravines, J. Dubois, J. D. Brion, M. Alami, Conformationally restricted naphthalene derivatives type isocombretastatin A-4 and isoerianin analogues: synthesis, cytotoxicity and antitubulin activity, *Eur. J. Med. Chem.* 52 (2012) 22-32.
- [22] D. Renko, E. Rasolofonjatovo, O. Provot, J. Bignon, J. Rodrigo, J. Dubois, J. D. Brion, A. Hamze, M. Alami, Rapid synthesis of 4-arylchromenes from ortho-substituted alkenols: A versatile access to restricted isocombretastatin A-4 analogues as antitumor agents, *Eur. J. Med. Chem.* 90 (2015) 834-844.
- [23] E. Rasolofonjatovo, O. Provot, A. Hamze, J. Rodrigo, J. Bignon, J. Wdzieczak-Bakala, C. Lenoir, D. Desravines, J. Dubois, J. D. Brion, M. Alami, Design, synthesis and anticancer properties of 5-arylbenzoxepins as conformationally restricted isocombretastatin A-4 analogs, *Eur. J. Med. Chem.* 62 (2013) 28-39.
- [24] M. Sriram, J.J. Hall, N.C. Grohmann, T.E. Strecker, T. Wootton, A. Franken, M.L. Trawick, K.G. Pinney. Design, synthesis and biological evaluation of dihydronaphthalene and benzosuberene analogs of the combretastatins as inhibitors of tubulin polymerization in cancer chemotherapy, *Bioorg. Med. Chem.* 16 (2008) 8161-8171.
- [25] C. Herdman, T.E. Strecker, R.P. Tanpure, Z. Chen, A. Winters, J. Gerberich, L. Liu, E. Hamel, R.P. Mason, D.J. Chaplin, M.L. Trawick, K.G. Pinney. Synthesis and biological evaluation of benzocyclooctene-based and indene-based anticancer agents that function as inhibitors of tubulin polymerization, *Med. Chem. Commun.* 7 (2016) 2418-2427.
- [26] R.P. Tanpure, C.S. George, M. Siram, T.E. Strecker, J.K. Tidmore, E. Hamel, A.K. Charlton-Sevcik, D.J. Chaplin, M.L. Trawicka, K.G. Pinney. An amino-benzosuberene analogue that inhibits tubulin assembly and demonstrates remarkable cytotoxicity, *Med. Chem. Commun.* 3 (2012) 720-724.
- [27] M. A. Soussi, O. Provot, G. Bernadat, J. Bignon, J. Wdzieczak-Bakala, D. Desravines, J. Dubois, J. D. Brion, S. Messaoudi, M. Alami, Discovery of Azaisoerianin Derivatives as Potential Antitumor Agents, *Eur. J. Med. Chem.* 78 (2014) 178-189.
- [28] M. A. Soussi, O. Provot, G. Bernadat, J. Bignon, D. Desravines, J. Dubois, J. D. Brion, S. Messaoudi, M. Alami, IsoCombretaQuinazolines: Potent Cytotoxic Agents with Antitubulin Activity, *ChemMedChem* 10 (2015) 1392-1402.
- [29] I. Khelifi, T. Naret, D. Renko, A. Hamze, G. Bernadat, J. Bignon, C. Lenoir, J. Dubois, J. D.; Brion, O. Provot, M. Alami, IsoCombretaQuinolines: Novel Microtubule Assembly Inhibitors with Potent Antiproliferative Activity, *Eur. J. Med. Chem.* 127 (2017) 1025-1034.
- [30] T. Naret, I. Khelifi, O. Provot, J. Bignon, H. Levaique, J. Dubois, M. Souce, A. Kasselouri, A. Deroussent, A. Paci, P. Varela, B. Gigant, M. Alami, A. Hamze, Diheterocyclic Ethylenes Derived from Quinaldine and Carbazole as New Tubulin Polymerization Inhibitors: Synthesis, Metabolism, and Biological Evaluation, *J. Med. Chem.* 62 (2019) 1902-1916.

- [31] I. Khelifi, T. Naret, T.; A. Hamze, J. Bignon, H. Levaique, C. Garcia, J. Dubois, O. Provot, M. Alami, *N,N*-bis-Heteroaryl Methylamines: Potent Anti-Mitotic and Highly Cytotoxic Agents, *Eur. J. Med. Chem.* 168 (2019) 176-188.
- [32] For a recent review on pyrido[1,2-*a*]indoles see: Y. Yao, M. Alami, A. Hamze, O. Provot, Recent advances in the synthesis of pyrido[1,2-*a*]indoles, *Org. Biomol. Chem.* 19 (2021), 3509-3526.
- [33] C. Jimenez, Y. Ellahioui, R. Alvarez, L. Aramburu, A. Riesco, M. Gonzalez, A. Vincente, A. Dahdouh, A.I. Mansour, C. Jimenez, D.M. Rogelio, G. Sarmiento, M. Medarde, R. Pelaez, Exploring the size adaptability of the B ring binding zone of the colchicine site of tubulin with para-nitrogen substituted isocombretastatins, *Eur. J. Med. Chem.* 100, (2015), 210-222.
- [34] T. Bzeih, T. Naret, A. Hachem, N. Jaber, A. Khalaf, J. Bignon, J.D. Brion, M. Alami, A. Hamze, A general synthesis of arylindoles and (1-arylvinyl)carbazoles via a one-pot reaction from *N*-tosylhydrazones and 2-nitro-haloarenes and their potential application to colon cancer, *Chem. Commun.* 52 (2016) 13027-13030.
- [35] T. Mandal, G. Chakraborti, S. Karmakar, J. Dash, Divergent and Orthogonal Approach to Carbazoles and Pyridinoindoles from Oxindoles via Indole Intermediates, *Org. Lett.* 20 (2018) 4759-4763.
- [36] J. Barluenga, P. Moriel, C. Valdés, F. Aznar, *N*-Tosylhydrazones as Reagents for Cross-Coupling Reactions: A Route to Polysubstituted Olefins. *Angew. Chem. Int. Ed.* 46 (2007) 5587-5590.
- [37] J. An, N.J. Chang, L.D. Song, Y.Q. Jin, Y. Ma, J.R. Chen, W.J. Xiao, Efficient and general synthesis of oxazino[4,3-*a*]indoles by cascade addition-cyclization reactions of (1*H*-indol-2-yl)methanols and vinyl sulfonium salts, *Chem. Commun.*, 47 (2011) 1869-1871.
- [38] G.C. Midya, A. Kapat, S. Maiti, J. Dash, Transition-Metal-Free Hydration of Nitriles Using Potassium *tert*Butoxide under Anhydrous Conditions. *J. Org. Chem.* 80 (2015) 4148-4151.
- [39] A. Giraud, O. Provot, A. Hamze, J.D. Brion, M. Alami. One-pot hydrosilylation-protodesilylation of functionalized diarylalkynes: A highly selective access to *Z*-stilbenes. Application to the synthesis of combretastatin A-4. *Tetrahedron Lett.* 49, 2008, 1107-1110.
- [40] This experiment (performed in triplicate) was reproduced by the same experimenter eight days apart to give the same disappointing result.
- [41] M.L. Shelanski, F. Gaskin, C.R. Cantor, Microtubule Assembly in the Absence of Added Nucleotides, *Proc. Natl. Acad. Sci. U.S.A.* 70, 1973, 765-768.
- [42] R.B. Lichtner, A. Rotgeri, T. Bunte, B. Buchmann, J. Hoffmann, W. Schwede, W. Skuballa, U. Klar, Subcellular distribution of epothilones in human tumor cells, *Proc. Natl. Acad. Sci. U. S. A.*, 98 (2001), 11743-11748.
- [43] M. A. Jordan, K. Wendell, S. Gardiner, W. Brent Derry, H. Copp, L. Wilson, Mitotic Block Induced in HeLa Cells by Low Concentrations of Paclitaxel (Taxol) Results in Abnormal Mitotic Exit and Apoptotic Cell, *Death Cancer Res.*, 56 (1996), 816-825.
- [44] IC₅₀ for doxorubicin against K562 and K562R is 0.44 mg/mL (800 μmol/L) and) 6.70 mg/mL (10⁻² mol/L), respectively. See: Pan, J. Leng, X. Deng, H. Ruan, L. Zhou, M. Jamal, R. Xiao, J. Xiong, Q. Yin, Y. Wu, M. Wang, W. Yuan, L. Shao, Q. Zhang. Nicotinamide increases the sensitivity of chronic myeloid leukemia cells to doxorubicin via the inhibition of SIRT1, *J. Cell. Biochem.* 121, 2020, 574-586.
- [45] H. Vakifahmetoglu-Norerg, A.T. Ouchida, E. Norberg, The role of mitochondria in metabolism and cell death, *Biochem. Biophys. Res. Commun.*, 482 (2017) 426-431.
- [46] J.B. Spinelli, M.C. Haigis, The multifaceted contributions of mitochondria to cellular metabolism, *Nat. Cell Biol.* 20 (2018) 745-754.
- [47] R. Huang, Y. Sheng, Z. Xu, D. Wei, X. Song, B. Jiang, H. Chen, Combretastatin A4-derived payloads for antibody-drug conjugates. *Eur. J. Med. Chem.* 216, (2021), 113355.
- [48] A. Maksimenko, M. Alami, F. Zouhiri, J.D. Brion, A. Pruvost, J. Mougin, A. Hamze, T. Boissenot, O. Provot, D. Desmaële, P. Couvreur, Therapeutic Modalities of Squalenoyl Nanocomposites in Colon Cancer: An Ongoing Search for Improved Efficacy, *ACS Nano*, 8 (2014), 2018-2032.
- [49] C. Venot, M. Maratrat, C. Dureuil, E. Conseiller, L. Bracco, L. Debussche, The requirement for the p53 proline-rich functional domain for mediation of apoptosis is correlated with specific PIG3 gene transactivation and with transcriptional repression, *EMBO J.* 17 (1998) 4668-4679.
- [50] E. F. Pettersen, T. D. Goddard, C. C. Huang, G. S. Couch, D. M. Greenblatt, E. C. Meng, T. E. Ferrin, UCSF Chimera-A visualization system for exploratory research and analysis. *J. Comput. Chem.* 25 (2004) 1605-1612.
- [51] <http://www.chemaxon.com>
- [52] O. Trott, A. J. Olson, AutoDock Vina: Improving the speed and accuracy of docking with a new scoring function, efficient optimization, and multithreading. *J. Comput. Chem.* 31 (2010) 455-461.